JOURNAL OF GEOPHYSICAL RESEARCH, VOL. 105, NO. B12, PAGES 27,917–27,938, DECEMBER 10, 2000

Crustal composition and mantle heat flow: Implications from surface heat flow and radiogenic heat production in the Variscan Erzgebirge (Germany)

Andrea Förster and Hans-Jürgen Förster
GeoForschungsZentrum Potsdam, Potsdam, Germany

Abstract. From an enlarged data set of temperature logs and thermal conductivity measurements, surface heat flow (q_s) in the Erzgebirge was determined to range from 61 to 112 mW m^{-2}. U-Th-K_2O data show that the heat flow pattern is controlled to first order by the occurrence of high heat production Variscan granites within a metamorphic basement. Highest heat flow correlates with granite plutons and sharply decreases off granite. These granites display variable but typically high radiogenic heat production (A), usually between 4 and 10 μW m^{-3}, depending on their chemical type and degree of fractionation. U accounts for 40–90% of the total heat production in the granites, whereas U and Th contribute equally to the radioactivity in the metamorphic basement. Compositional heterogeneity in the upper crust, owing to variation of conductive heat transfer, required corrections of measured surface heat flow up to 20 mW m^{-2}, depending on location of the heat flow site. Heat budget calculations, considering crustal models derived from seismic and gravimetric surveys, define the thickness (D) of crust enriched in radioactive elements to 15 km, the rate of reduced heat flow (q^*) to 30–34 mW m^{-2}, and the mantle heat flow to 20–30 mW m^{-2}, in contradiction to what is implied from q_s-A plots. In fact, D (5–8 km) and q^* (45–52 mW m^{-2}) from these plots represent the thickness of, and the heat flow beneath, the (granite) layer that is most enriched in heat-producing elements. For a crustal section strongly heterogeneous in upper crustal heat production, traditional interpretation of q_s-A plots is misleading and should be supplemented routinely by heat budget calculations.

1. Introduction

The Erzgebirge is part of the Central European Variscides and is situated in the southern belt of the Saxothuringian zone [e.g., *Matte et al.*, 1990], at the northwestern edge of the Bohemian massif (Figure 1, inset map). The area consists of metamorphic rocks of Proterozoic and Paleozoic protolith age invaded by voluminous masses of shallowly emplaced, evolved granites [*Tischendorf et al.*, 1965], most of which are placed into the high heat production (HHP) category. The Erzgebirge is bound by the Fichtelgebirge anticline to the southwest and the Elbe lineament to the northeast. Northwest of the Erzgebirge anticline are synclines and basins composed of Paleozoic sediments. The Erzgebirge extends to the south into the Czech Republic and there is named the Krušné hory mountains.

In the last several decades the area has undergone intensive surveys for, and exploitation of, mineral deposits (Sn, W, U, Pb, Zn, F, Ba). As a result, substantial amounts of data on the geologic history, prevailing rock types, and ore deposits are available from surface outcrops, underground mines, and exploration wells [*Tischendorf and Förster*, 1994]. Geophysical investigations comprising gravity, electric, and seismic surveys were used to characterize the structure and composition of the crust down to the Moho (see *Behr et al.* [1994] for a summary).

Prior to these geophysical studies, terrestrial heat flow was described as forming a complex pattern [see *Oelsner and Hurtig*, 1979; *Hurtig and Oelsner*, 1979, and references therein]. It was reported that high heat flow, of the order of 90–92 mW m^{-2} in local anomalies, alternated with lower heat flow, between 27 and 38 mW m^{-2}. Somewhat modified heat flow data were presented in the framework of the geothermal atlas of the German Democratic Republic [*Diener et al.*, 1984] and in the geothermal atlas of Europe [*Hurtig and Rockel*, 1992]. Although the heat flow data were few and unevenly distributed, machine contouring was used for mapping, resulting in patterns that were only poorly understood. High values were attributed to the rejuvenation of major tectonic, deep-reaching lineaments, whereas the general irregular heat flow pattern was interpreted as a reflection of different degrees of deformation of the crust. Heat production in the granites and their metamorphic country rocks remained unconsidered.

Previous heat flow studies, which relied partly on temperature data measured in mines and partly on continuous temperature logs obtained in boreholes, lacked detailed description of the basic data used. Moreover, the methodology of determining heat flow was not described. So, questions were raised whether signals of fluid flow perturbations were overlooked in the subsurface temperature data and whether the thermal conductivity of metamorphic rocks influenced the variability of heat flow. Altogether, interpretation of the positive heat flow anomalies (enhanced mantle heat flow, crustal composition, deep-reaching fluid flow or a combination of these effects) remained flawed, limiting the significance of previous models of the thermal state of the Erzgebirge crust [*Oelsner*, 1978; *Wagner*, 1989]. With regard to these shortcomings it seemed appropriate to revisit the heat flow problem in the Erzgebirge.

Paper number 2000JB900279.
0148-0227/00/2000JB900279$09.00

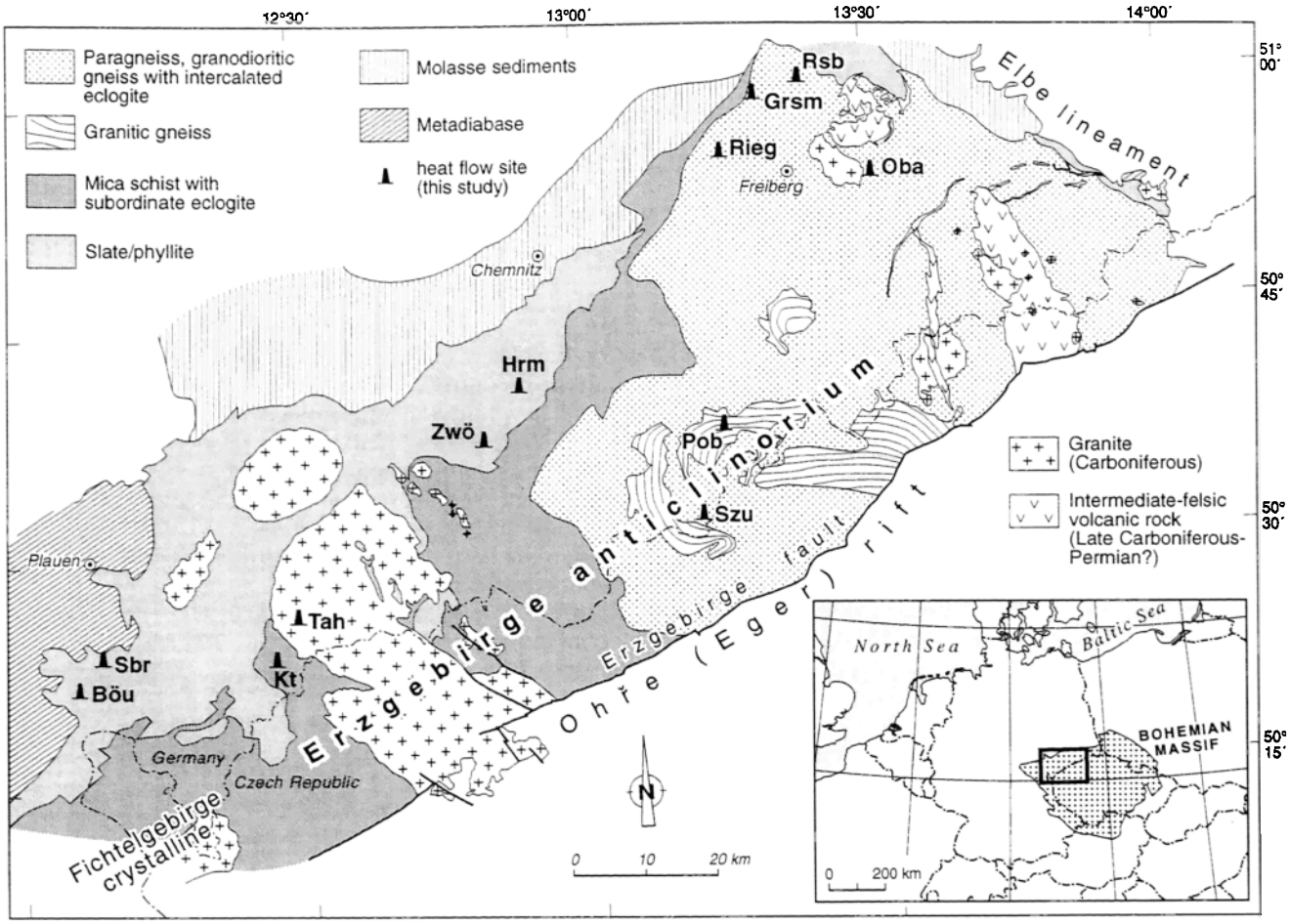

Figure 1. Generalized geological map of the Erzgebirge (modified from geological maps of the *Sächsisches Landesamt für Umwelt und Geologie* [1995] and *Willner et al.* [1997]). Borehole sites used for heat flow determination are shown. Böu, Bösenbrunn; Sbr, Schönbrunn; Kt, Klingenthal; Tah, Tannenbergsthal; Zwö, Zwönitz; Hrm, Hormersdorf; Pob, Pobershau; Szu, Satzung; Rieg, Riechberg; Grsm, Großschirma; Rsb, Reinsberg; Oba, Obergruna.

Our goals were (1) to revise and update the heat flow regime, (2) to discuss heat flow in the context of new results on radiogenic heat production in granitic and metamorphic rocks and with regard to crustal structure as deduced from geophysical studies, and (3) to compare the thermal structure of the Erzgebirge with that of other well-studied areas such as the Armorican massif (western France) and SW England (Cornwall), which are considered to represent typical European Variscan crust. Special attention is paid to the ability of the heat flow/heat production relation to infer the distribution of heat production in the continental crust.

2. Geological Setting

The Erzgebirge constitutes a large NE trending antiformal megastructure built up by a variegated suite of metamorphic rocks of early Carboniferous age (~350–330 Ma) which represents a tectonic stack of units that experienced different metamorphic conditions [*Willner et al.*, 1997; *Kröner and Willner*, 1998; *Mingram*, 1998; *Rötzler et al.*, 1998]. Its core is composed of medium- to high-grade mica schist, paragneiss, granodioritic as well as granitic orthogneiss, and local intercalations of mafic amphibolite, eclogite, and rare garnet peridotite bodies (Figure 1). This assemblage of rocks of Proterozoic/Paleozoic protolith age tectonically is overlain and surrounded to the north and to the west by a NE trending phyllite unit containing very low- to low-grade metamorphic rocks. In the southwest this phyllite unit borders on upper Devonian mafic volcanic rocks (ash-lapilli tuff and metadiabase) intercalated with graywacke, shale/slate, and limestone, which overlie Silurian to lower Carboniferous units, mostly slate and sandstone [*Kuschka and Hahn*, 1996].

The following Variscan stages in assemblage of the Erzgebirge crust can be established: (1) peak metamorphism (eclogite facies) of Paleozoic rocks at 350–340 Ma, (2) followed by rapid uplift and cooling (340–326 Ma), (3) an erosional unconformity with deposition of sediments at 326 Ma, and (4) intrusion of oldest (late collisional) granites and lamprophyres at 325 Ma [see *Förster et al.*, 1999, and references therein]. The basement rocks were invaded by a second pulse of postcollisional granitic melts during the late Carboniferous and early Permian (~310–285? Ma). Tertiary block faulting produced differential uplift such that penecontemporaneous rhyolithic and rhyodacitic lavas and subvolcanic dikes are exposed only in the eastern Erzgebirge.

Morphologically, the Erzgebirge constitutes a northwesterly dipping fault block with elevations that rise gradually from

Table 1. List of Erzgebirge Boreholes >150 m Depth, in which Temperature Logs Are Available

Borehole Designation	Longitude °E	Latitude °N	Collar Elevation, m	Borehole Diameter, mm	Total Depth, m	Number of Logs	Logging Date
Böu 5/73	12.087	50.407	465	113	350	2	Jan. 2, 1974
Böu 7/74	12.094	50.402	424	86	198	1	May 28, 1974
Böu 9	12.095	50.403	403	86	500	1	March 13, 1975
Böu 16/77	12.101	50.400	441	93	715	1	Sept. 13, 1977
Böu 37/76	12.097	50.402	399	76	502	2	July 21, 1976
Grsm 1/76	13.284	50.974	365	93	400	2	April 12, 1976
Grsm 2/77	13.289	50.971	356	76	1200	2	Aug. 29, 1978
Hrm 1E/75	12.858	50.661	513	76	365	2	Nov. 28, 1975
Jac 22/74	12.905	50.654	655	76	304	1	May 30, 1974
Jac 23/74	12.873	50.642	677	76	270	1	July 17, 1974
Jac 24/74	12.871	50.649	671	76	181	1	July 30, 1974
Kt 1/78	12.485	50.367	754	76	500	1	July 10, 1978
Kt 2/78	12.487	50.352	731	76	1080	1	March 10, 1979
Kt 3/78	12.464	50.372	599	76	500	2	Sept. 25, 1978
Kt 8/82	12.426	50.416	745	76	595	2	Sept. 2, 1982
Kt 18/81	12.435	50.403	814	76	781	2	Dec. 3, 1981
Kt 34/81	12.440	50.402	820	76	934	3	Oct. 26, 1981
Oba 1/77	13.313	51.001	309	76	300	1	Oct. 11, 1977
Pob 1/78	13.225	50.632	662	76	731	2	Aug. 17, 1978
Pob 2/79	13.211	50.634	628	76	767	2	Sept. 14, 1979
Rieg 1/76	13.199	50.928	381	76	702	2	July 31, 1976
Rsb 1/77	13.371	50.991	344	76	698	1	Dec. 14, 1977
Sbr 2/74	12.107	50.417	484		418	1	Oct. 10, 1974
Sbr 4/75	12.109	50.418	485	86	703	1	Sept. 30, 1975
Sbr 5/74	12.110	50.418	474		567	1	Feb. 1, 1975
Sbr 6/75	12.114	50.417	455	86	770	1	Oct. 31, 1975
Sbr 7/73	12.115	50.415	460	101	948	4	Jan. 2, 1974
Sbr 8/74	12.117	50.413	467	86	649	1	March 20, 1975
Sbr 9/73	12.119	50.412	451	101	900	5	Nov. 22, 1973
Sbr 10/76	12.113	50.416	463	93	880	1	Nov. 8, 1977
Sbr 14/74	12.125	50.404	473	86	545	1	March 21, 1975
Sbr 16/76	12.109	50.419	451	93	928	2	July 14, 1976
Szu 1/78	13.191	50.519	867	76	868	2	Nov. 23, 1978
Tah 4/77	12.486	50.425	827	76	1200	1	Feb. 28, 1978
Tah 13/80	12.491	50.424	818	76	859	3	Sept. 16, 1980
Tih 1	12.649	50.807	349		490	1	March 22, 1963
Waba IIA/62	13.083	50.661	451			2	Aug. 7, 1962
Waba III/62	13.083	50.661	450			1	June 18, 1963
Zwö 1/78	12.819	50.615	646	76	751	2	May 29, 1978

Böu, Bösenbrunn; Grsm, Großschirma; Hrm, Hormersdorf; Jac, Jahnsbach; Kt, Klingenthal; Oba, Obergruna; Pob, Pobershau; Rieg, Riechberg; Rsb, Reinsberg; Sbr, Schönbrunn; Tah, Tannenbergsthal; Tih, Tirschheim; Waba, Warmbad; Zwö, Zwönitz.

northwest to southeast, from the Erzgebirge depression in the foreland near Chemnitz (300 m above sea level) toward the Erzgebirge anticlinorium (800–1000 m on average near the Erzgebirge ridge). To the southeast the area is bounded by the Erzgebirge fault, which constitutes the northwestern border of the Ohře (Eger) rift in which granites compositionally equivalent to those in the study area occur.

3. Temperature Logs

Compared to the large number of boreholes drilled in connection with the extensive search for mineral deposits between 1960 and beginning of the 1980s, holes in which temperature logs were obtained are scarce. These boreholes range in depth from several hundred meters to a maximum of 1200 m. The borehole locations with thermal logs are listed in Table 1. The data include the borehole name, location, collar elevation, hole diameter, total depth of the borehole, number of temperature logs obtained, and logging date. Table 1 lists all measurements compiled and accessible for this study. Although not explicitly stated, some of the boreholes listed in Table 1 (Rieg 1, Grsm 1, Rsb 1, Sbr, and Böu) were included in the previous contoured heat flow map [*Oelsner and Hurtig*, 1979], but no details on their log interpretation were given.

Because the wells were drilled for exploration and the thermal logs were measured commercially, the prerequisites for a high-quality heat flow analysis as known from scientific wells were not met. Also, new temperature measurements in these wells were impossible because all were plugged. For most of the boreholes the logging date and the time they were left undisturbed after cessation of drilling (shut-in time) are available. However, it is not possible to check how reliable these data are because of lack of information of when the last circulation of borehole fluid was performed. Because many of the logs were obtained for the purpose of recognizing short-term thermal perturbations associated with fluid flow in higher permeability joints and faults of mineralized zones, the shut-in time of the wells usually was only of the order of several hours. On the other hand, there are some wells in which temperature logs were measured after a considerably longer shut-in time so that the values are close to equilibrium temperature. Some of the wells have thermal logs repeatedly measured at different shut-in times so that a general correction factor for thermal disturbances due to drilling was constrained and applied to wells with short shut-in times.

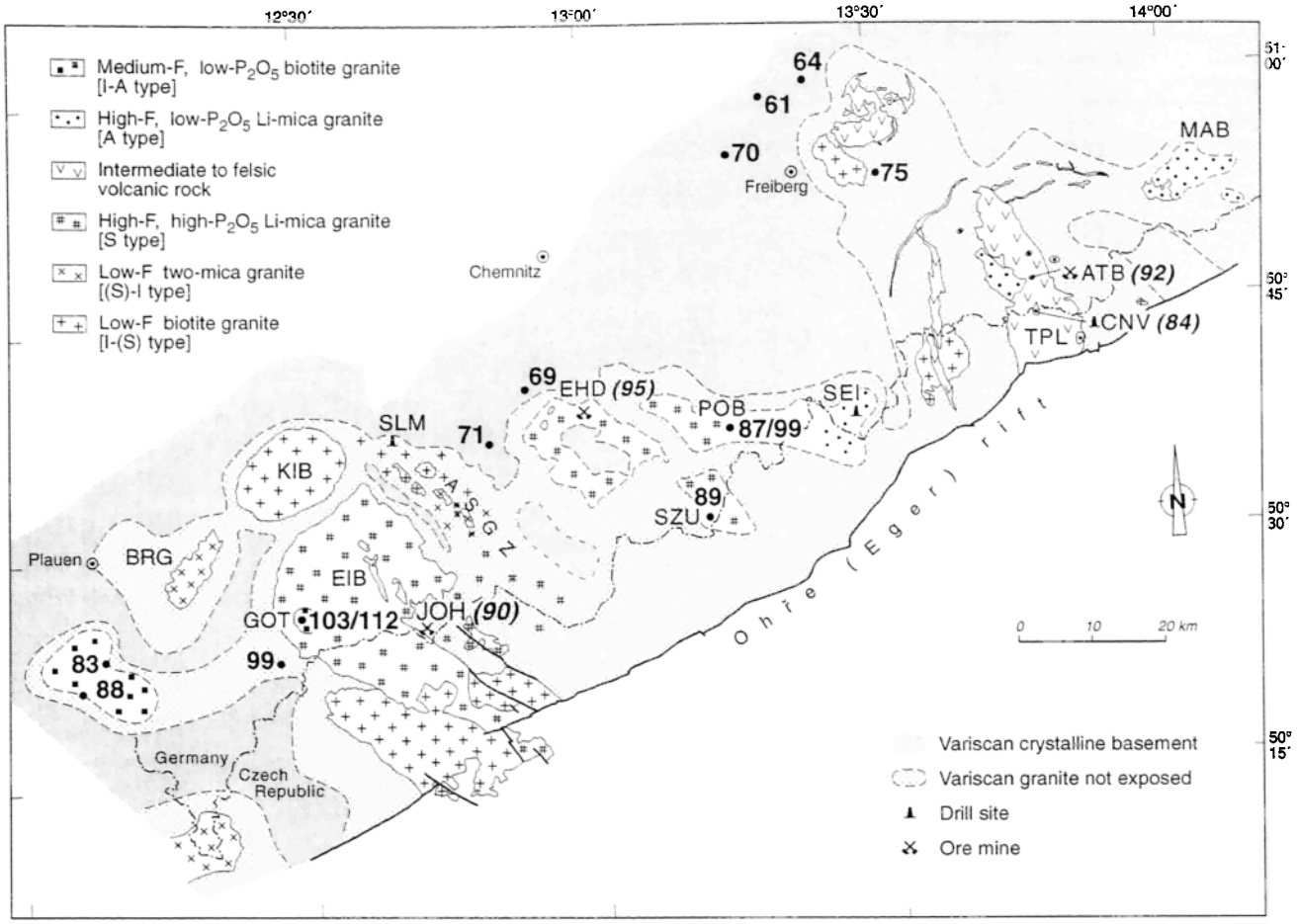

Figure 2. Geological map of the Erzgebirge showing the distribution of the various types of Variscan granitic and volcanic rocks (modified from *Förster et al.* [1999]) in conjunction with heat flow data (in mW/m^2) from this study (bold) and previous works (in italics; see text). ATB, Altenberg; EHD, Ehrenfriedersdorf; JOH, Johanngeorgenstadt; KIB, Kirchberg; BRG, Bergen; GOT, Gottesberg; EIB, Eibenstock; CNV, Cinovec; SEI, Seiffen; MAB, Markersbach; TPL, Teplice; POB, Pobershau; SZU, Satzung.

Analysis and correction of temperature logs are given in Appendix A. Care was taken to select for heat flow analysis thermal profiles from those wells that seem not to be affected by fluid flow. Although disturbed temperature-depth curves provide information on hydraulic activity [e.g., *Brott et al.*, 1981; *Blackwell*, 1989; *Kukkonen*, 1995], our objective is to define the heat conduction component of heat transfer, which reduced the number of boreholes and depth intervals suitable for heat flow interpretation.

4. Thermal Conductivity

Thermal conductivity and the geothermal gradient are the two quantities that control the heat flow density according to Fourier's law of heat conduction. It is important to assess the thermal conductivity (λ) accurately because an order of magnitude change in this parameter affects the final heat flow value to a greater extent than a gradient change of the same amount. λ measurements were made on core samples from the drill holes in which temperature logs were made or are from wells in close proximity. Unfortunately, availability of core material was limited, and no complete λ profiles could be determined. The measurements were made on dry air core samples under room temperature, using alternatively the divided-bar method and the optical-scanning method (for details of these techniques, see *Popov et al.* [1999]). Additional information on thermal conductivity measurements is provided in Appendix B.

Table A1 summarizes data for major rock types. Phyllite and slate show similar thermal conductivity. Pelites fall into the phyllite/slate category but show no anisotropy. The anisotropy ratios are in the range of values reported by other authors (see *Schön* [1996] for a summary). Orthogneiss and paragneiss show a similar ratio of anisotropy. Granite thermal conductivity was measured on samples from the Tah 4 and the Pob 2 boreholes. The Pobershau granite yields 3.6 $W\ m^{-1}\ K^{-1}$, whereas the Gottesberg granites show some variability, with values between 3.3 and 3.8 $W\ m^{-1}\ K^{-1}$, which is likely the result of hydrothermal alteration, as described by *Wasternack et al.* [1995]. Table A2 lists for each depth interval of temperature gradient the mean thermal conductivity assigned.

5. Radiogenic Heat Production

Knowledge of the abundances of heat-producing elements (HPE) in the Variscan igneous rocks and their metamorphic country rocks is extensive and permits detailed insight into the distribution pattern of radiogenic heat production (A) within the Erzgebirge crust. Heat production was calculated accord-

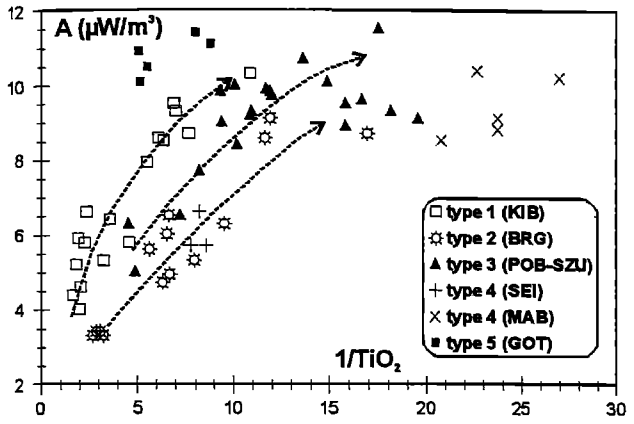

Figure 3. Heat production (A) in unaltered Variscan Erzgebirge granites as function of granite type and degree of fractional crystallization differentiation (expressed by $1/TiO_2$ in whole rock). Plutons representing the granite types 1–5 (see text) are given in parentheses and are abbreviated as follows: KIB, Kirchberg; BRG, Bergen; POB-SZU, Pobershau-Satzung; SEI, Seiffen; MAB, Markersbach; GOT, Gottesberg. See Figure 2 for location of the granites. Sources of U-Th-K whole rock data: KIB, BRG, POB-SZU [*Förster et al.*, 1999]; MAB, SEI (H.-J. Förster, unpublished data, 1999); GOT [*Gottesmann et al.*, 1995]. Arrows indicate increase of radiogenic heat production with progressive magma differentiation in the KIB, BRG, and POB-SZU cogenetic granite series.

ing to the equation of *Rybach* [1973], using rock density values of Erzgebirge rocks determined by *Kopf* [1961]. The analytical methods of HPE determination in whole rock samples are reported in Appendix C.

5.1. Variscan Magmatic Rocks

Granites predominate in volume to volcanic rocks (see Figure 2), and thus their radiogenic heat production should control the surface heat flow patterns. These peraluminous granites are compositionally heterogeneous and are classified into five major types [*Förster et al.*, 1998]: (1) low-F biotite granites of transitional I-S type [SiO_2(wt %) = 66.8–77.4; A(μW m^{-3}) = 5.6 ± 1.9, n = 91]; (2) low-F two-mica granites of transitional S-I type (SiO_2 = 70.6–76.6; A = 5.3 ± 2.0, n = 21); (3) high-F, high-P_2O_5 Li-mica granites of S-type affinity

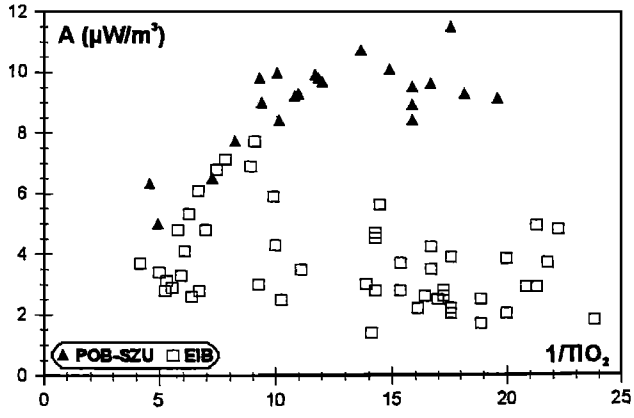

Figure 4. Heat production in drill core samples (Pobershau-Satzung, POB-SZU) and surface samples (Eibenstock, EIB) of S-type Li-mica granites (modified from *Förster et al.* [1998]).

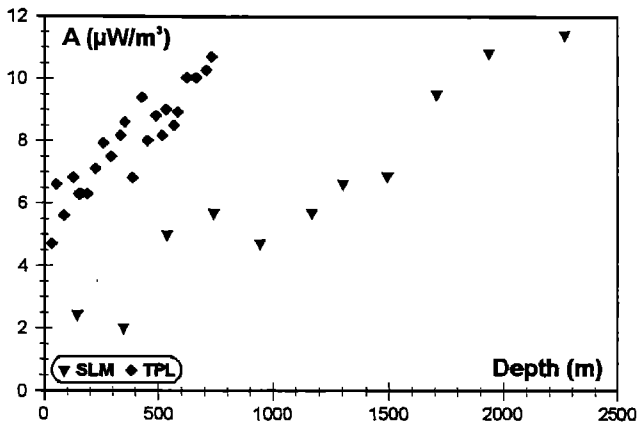

Figure 5. Variation of heat production with depth in the low-F biotite granite of Schlema-Alberoda (SLM) and the Teplice rhyolite suite (TPL). A in SLM granites was calculated using U-Th-K data from *Barsukov et al.* [1996]. A for TPL is from *Ostřihanský* [1988].

(SiO_2 = 72.3–76.8; A = 8.0 ± 2.3, n = 59]; (4) high-F, low-P_2O_5 granites of aluminous A-type affinity (SiO_2 = 71.9–76.9; A = 8.9 ± 2.0, n = 60), and (5) moderate- to high-F biotite granites of mixed A-I type (SiO_2 = 72.7–76.4; A = 10.1 ± 0.7, n = 11). Furthermore, the granites form composite plutons containing a variety of geochemically distinct subintrusions, which are genetically related via fractional crystallization.

Radiogenic heat production in the granites, fresh and altered, ranges from 1 to 16 μW m^{-3}, with most determinations between 4 and 10 μW m^{-3}. Variability in A depends on a number of factors of which the following are most important: (1) type of granite, (2) degree of fractionation, and (3) intensity of alteration. Well-studied plutons are selected to demonstrate these relations (Figures 3–5).

Irrespective of type, radiogenic heat production in unaltered granites increases with magmatic differentiation (Figure 3). However, the granites achieve their maximum heat production at distinctly different degrees of fractionation. Extremes are displayed by the Gottesberg suite (representative of type 5 granites), where only moderate fractionation was required, and the Markersbach intrusion (representative of type 4 granites) which is distinguished by a high level of differentiation. Furthermore, the granite types also differ slightly in the minimum radiogenic heat production typical for least fractionated intrusions. Among type 1 and type 2 granites, intrusions occur exhibiting radiogenic heat production values as low ~3 μW m^{-3}. In contrast, Li-mica granites of types 3 and 4 having radiogenic heat production values <3.5 and 5 μW m^{-3}, respectively, are unknown in outcrop.

The pronounced effect of alteration on radiogenic heat production is best exemplified by comparing radiogenic heat production in samples from surface exposures and drill cores from Li-mica granites of the S type (Figure 4). As demonstrated by *Förster et al.* [1998], nearly geochemically identical granites have significantly different U contents depending on whether they outcrop (Eibenstock) or are buried (Pobershau-Satzung). In the Erzgebirge, samples collected from surface outcrops have lost between 2 and 5 times their initial U contents, most likely the result of leaching processes involving oxidized meteoric or hydrothermal waters [e.g., *Tischendorf and Förster*,

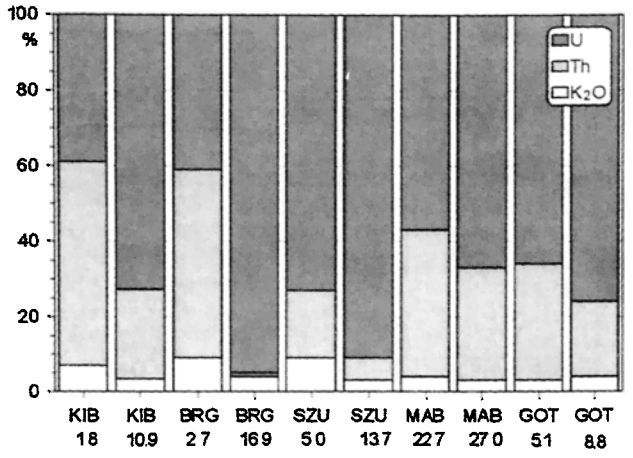

Figure 6. Relative contribution of U, Th, and K_2O to total heat production in low- and high-fractionated subintrusions of composite plutons of type 1–5 granites. See Figure 3 for abbreviations. Numbers on the x axis refer to $1/TiO_2$ in whole rock.

1994]. Given the major contribution of U to the entire budget of heat-producing elements, heat production of surface samples may be up to 5 times lower than that in unleached portions of the pluton.

Moreover, granitic and rhyolitic rocks are known in which an increase in U with depth is accompanied by a simultaneous increase in Th. Increase of U with depth reflects the decreasing intensity of U leaching. Uranium depletion due to leaching occurs to depths of some hundred meters or, in case of the Schlema-Alberoda granite, to >2 km [*Ostřihanský*, 1988; *Barsukov et al.*, 1996]. Decrease of Th toward the surface is the result of magma differentiation due to fractionation of monazite and thorite, giving rise to Th-depleted, more differentiated granites. These granite subintrusions are preferentially located in the upper parts of multiphase plutons which, in the Erzgebirge, are at or near the recent level of erosion. The simultaneous increase of both elements causes an increase of heat production with depth that is more pronounced than the effect on heat production by U leaching alone (Figure 5). For example, in the Schlema-Alberoda granite, heat production of samples from 2300 m depth is 6 times higher than that of samples collected near to the surface.

Heat production in granitic rocks is governed mainly by U and Th, which usually make up >90% of the total heat production (Figure 6). Potassium is of subordinate importance, contributing from ~10–13% in least evolved granites to <5% in strongly evolved intrusions. Uranium exerts a major control on heat production in almost all granites, with a proportion ranging from 40 to 90%, increasing with progressive magmatic differentiation. The reverse trend is established for Th, which dominates over U only in the most primitive biotite and two-mica granites of types 1 and 2.

Mass balance calculations indicate that about 90% of U and Th in type 1–3 granites is bound in accessory minerals [*Förster*, 1998]. Between 30 and 90% of the U is fixed in uraninite. The remaining U is contained in monazite, xenotime, zircon, and, if present, thorite. Each of the latter phases account for <20% of the U budget. In the two-mica and Li-mica granites, uraninite occurs as a low-Th variety which, if not protected from fluid infiltration, is easily soluble [e.g., *Förster*, 1999]. Destruction of abundant Th-poor uraninite by low-T solutions explains the depletion of U in the superficially exposed Eibenstock Li-mica granite pluton shown in Figure 4 and the Schlema-Alberoda biotite granite portrayed in Figure 5 [*Förster et al.*, 1998; *Förster*, 1999]. In contrast, in other biotite granites of the area, such as the Kirchberg pluton, a Th-rich uraninite occurs, which is highly resistant against destabilization. In these granites, both surface or altered samples have roughly similar heat production.

In the vast majority of granites the dominant host of Th is monazite, which accounts for 80–90% of the Th budget. Where monazite is absent, allanite plus thorite are the most important carriers of Th (~80%). If present, thorite is responsible for 30–50% of total Th. Although allanite and thorite display strong metamictization [*Förster et al.*, 1999] and granitic monazite may experience leaching of Th when attacked by a fluid phase [*Poitrasson et al.*, 1996; *Broska et al.*, 2000], the released Th is usually redeposited into newly formed secondary phases next to its source in most granites from the Erzgebirge and elsewhere [see *Förster*, 2000, and references therein]. These observations explain why Th concentrations in granites are mostly unrelated to intensity of alteration [e.g., *Irber*, 1999]. However, this does not hold for all granites. For example, in some of the type 5 granites in the Erzgebirge, enhanced Th mobility is observed at the scale of decimeters or meters (H.-J. Förster, unpublished data, 2000).

Reliable mass balance assessments for types 4 and 5 granites are difficult to perform because a couple of other minerals such as pyrochlore, U-bearing tantalo-niobates, Th-bearing fluorocarbonates, etc., occur in the accessory mineral assemblage to variable degrees. However, U and Th behavior is principally governed by the same factors as in the formerly discussed types.

Although granites rich in Th [e.g., *Eby*, 1990; *Frost et al.*, 1999], in U [*Kontak*, 1990], or both [*Taylor*, 1992; *Chappell*, 1999] are known worldwide, they are particularly abundant in the Erzgebirge. This can be shown by plotting samples from unleached Erzgebirge granites (German part) relative to various granite averages [*Whalen et al.*, 1987; *Condie*, 1993] in U/Th space (Figure 7). Thus heat production of the vast ma-

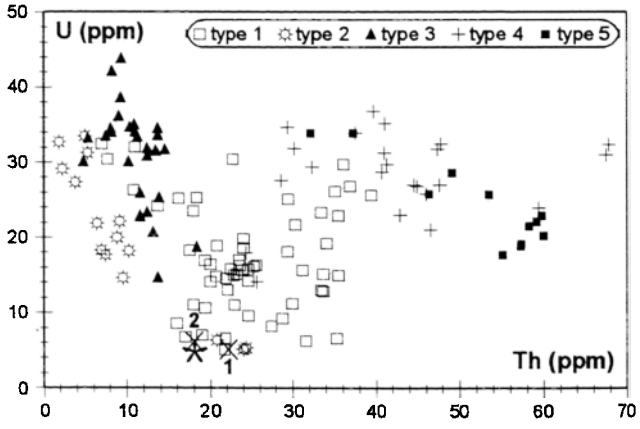

Figure 7. U versus Th plot for unleached granites from the Erzgebirge. Asterisk indicates average of Phanerozoic granite (73.8 wt % SiO_2) according to *Condie* [1993]. Crosses mark averages of felsic (73.4 wt % SiO_2) I-type (1) and S-type granites (2) from the Lachlan Fold Belt in Australia [*Whalen et al.*, 1987].

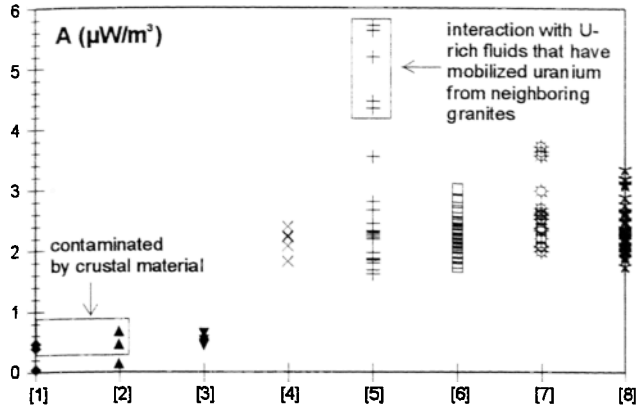

Figure 8. Heat production of metamorphic rocks from the Erzgebirge: 1, eclogite; 2, mafic amphibolite; 3, metadiabase; 4, metagranodiorite; 5, metagranite; 6, paragneiss; 7, mica schist; 8, phyllite. Data are from *Mingram* [1996] and this study.

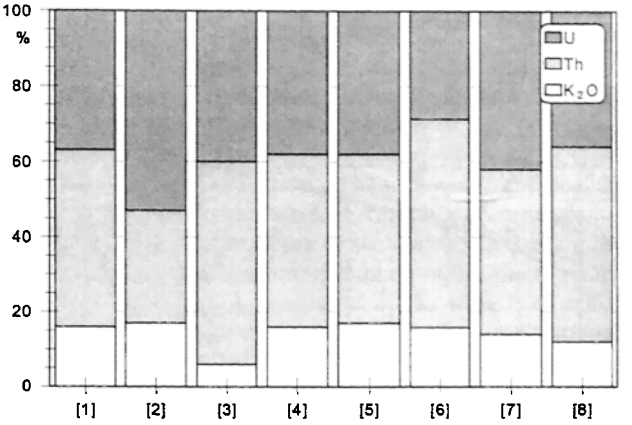

Figure 9. Relative contribution of U, Th, and K_2O to heat production in metamorphic rocks: 1, eclogite; 2, mafic amphibolite; 3, metadiabase; 4, metagranodiorite; 5, metagranite; 6, paragneiss; 7, mica schist; 8, phyllite.

jority of granites exceeds that of average Phanerozoic granite (2.8 μW m^{-3}) and average felsic I- and S-type granites (3.0 μW m^{-3}).

5.2. Early Variscan Metamorphic Basement Rocks

The major types of metamorphic rocks display a relatively narrow range in radiogenic heat production (Figure 8). Mafic rocks including eclogite, amphibolite, and metadiabase have A values <0.5 μW m^{-3}. Radiogenic heat production of upper crust metamorphic rocks, irrespective of whether they are orthometamorphic or parametamorphic, ranges between 1.5 and 3.5 μW m^{-3}, with the majority of values between 2 and 3 μW m^{-3}.

In contrast to the Variscan granites, heat production in metagranodiorite (biotite gneiss) and metagranite (muscovite gneiss) shows little variation with degree of magmatic fractionation. In the boreholes studied, heat production of these rocks remains fairly constant over the entire depth profile. However, muscovite gneisses from the Satzung/Pobershau heat flow sites demonstrate that metamorphic rocks in close proximity to leachable granites may have suffered from interaction with U-rich material (Figure 8). Here hydrothermal fluids have mobilized U from the neighboring granites, which then was redeposited into the gneisses partly as pitchblende along fractures or as other U phases along grain boundaries. Secondary U enrichment resulted in heat production that is between 2 and 3 times higher than that of the original rock. Contamination of crustal material is the likely source of the heat production increase observed in some mafic metamorphic rocks shown in Figure 8.

Although the contribution of K_2O to the heat production budget of the metamorphic rocks is slightly higher than in the Variscan granites, it is still subordinate to U and Th (<20%), which account for 30–50% of the budget, respectively (Figure 9).

The limited variability in heat production of the Erzgebirge metamorphic rocks is readily explainable by their particular suite of radioactive accessory minerals and by susceptibility of the latter to metamorphic or hydrothermal reworking. Although no detailed study of accessory minerals has been undertaken, uraninite was not detected in any of the different metamorphic rocks. Furthermore, there is accumulated evidence either that, in general, the major hosts of the radioactive elements (monazite, zircon, apatite ± xenotime ± Th orthosilicate) in intermediate to felsic igneous rocks or paragneisses remain stable during interaction with a fluid phase or that leached Th and U abundances were mobilized over short distances only [see *Bingen et al.*, 1996; *Finger et al.*, 1998; *Broska and Siman*, 1998].

Although less extreme than the Variscan granites, the different upper crustal basement rocks of the Erzgebirge are also enriched in Th and U compared to well-established global averages (Figure 10). Most samples from the major types of parametamorphic rocks (groups 5–7) contain Th and U in abundances that exceed those in average Phanerozoic graywacke and shale [*Condie*, 1993]. They are also enriched compared to loess and post-Archean Australian shale (PAAS) [*Taylor and McLennan*, 1985] suggested to approximate the

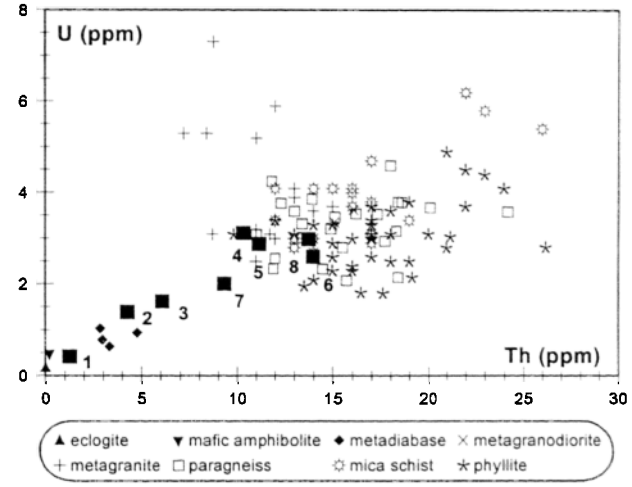

Figure 10. U versus Th plot for metamorphic rocks from the Erzgebirge: 1, lower continental crust [*Taylor and McLennan*, 1985]; 2, bulk continental crust [*McLennan and Taylor*, 1996]; 3, middle continental crust [*Rudnick and Fountain*, 1995]; 4, upper continental crust [*Taylor and McLennan*, 1985]; 5, average PAAS [*Barth et al.*, 2000]; 6, average loess [*Barth et al.*, 2000]; 7, average Paleozoic graywacke [*Condie*, 1993]; 8, average Paleozoic shale [*Condie*, 1993].

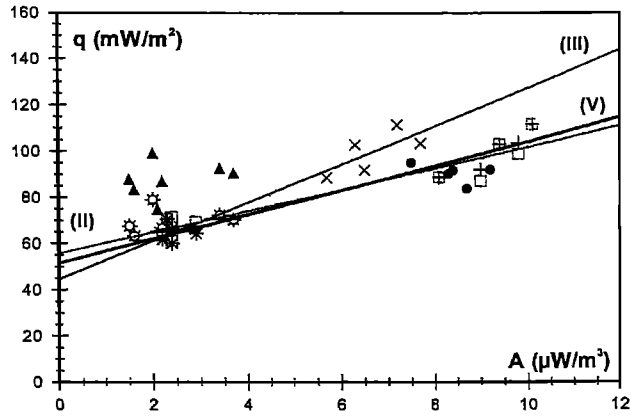

Figure 11. The q_s-A plots for the Erzgebirge. Curve II is fit of values measured in granites and metamorphic rocks outside the granite area (open squares); curve III is fit of values from the same heat flow sites, but q is corrected for lateral heat conduction disturbance (pluses); curve V is same as curve II but for A of granites representing minimum radioactive heat production characterizing the least fractionated granites of plutons (crosses). Solid triangles denote q_s-A pairs measured in metamorphic rocks within the area of granite distribution. The respective q values corrected for vertical heat flow disturbance are shown as sunbursts. Dots indicate the q_s-A relationships measured in underground mines in granites (ATB, EHD, JOH; q_s is from *Oelsner and Hurtig* [1979] and A is from this study) and from boreholes in the Cinovec granite in the Czech Erzgebirge [see *Ostřihanský*, 1988, Table 1]. See text for detailed explanation.

average composition of the upper continental crust [*Taylor and McLennan*, 1985].

6. Surface Heat Flow

6.1. Regional Heat Flow Pattern

Analysis of surface heat flow (q_s) is elaborated in Appendix D. Table A2 provides the basic geothermal data and results. Evaluation of the regional q_s patterns indicates that highest heat flow (87–112 mW m^{-2}) occurs within or adjacent to the granite plutons (see Figure 2). These values are in good agreement with previous data determined in underground mines within granite plutons (90–95 mW m^{-2}) and the heat flow measured in the Cinovec granite in the Czech Erzgebirge (84 mW m^{-2}) (Figure 11).

The heat flow patterns in metamorphic rocks also show close spatial relations to the distribution of Variscan granites. Two groups can be distinguished: (1) values in the range of 61–71 mW m^{-2} from sites outside the area of overall granite occurrence (off-granite heat flow) and (2) higher values of the order of 75–99 mW m^{-2} from sites in the vicinity of granite plutons.

The range of surface heat flow from group 1 heat flow sites, which shows variations of up to ±5 mW m^{-2}, can easily be explained by heat refraction and anisotropy as a result of variable inclination of foliation and bedding in the metamorphic units and thus may be considered as the potential error in the heat flow determination in these rock types. Unfortunately, the large-scale and small-scale structure of the subsurface around the boreholes is not known to an extent that would help to resolve the pattern of heat conduction through the anisotropic metamorphic rock. One example, showing the quantities of perturbations of conductive heat flow resulting from structural anisotropy in the upper crust, is provided by *Bayer et al.* [1996] using finite element calculations in their study of the Variscan front near Aachen (Germany). Their two-dimensional (2-D) model shows vertical and lateral heat flow anomalies of the order of 3–10 mW m^{-2}. *Kukkonen and Šafanda* [1996] report, from crystalline rocks in Finland, differences between isotropic and anisotropic 2-D finite difference models in the range from −2.6 to 3.9 mW m^{-2}. However, the difference between off- and on-granite surface heat flow in the study area is between 4 and 38 mW m^{-2} and exceeds the range of variations attributable to anisotropy alone. Close spatial relations of group 2 heat flow sites to Variscan granites suggest that their elevated heat flow is related to the high radiogenic heat production of the granites and thus is not truly representative of the metamorphic rock units, as will be demonstrated in section 6.2.

6.2. Effects of Radiogenic Heat Production Contrasts on Heat Flow

The effects of horizontal heat conduction due to variations in radiogenic heat production have been addressed in several papers in the past [e.g., *England et al.*, 1980; *Jaupart*, 1983; *Furlong and Chapman*, 1987]. It was recognized and proved by modeling that sharp radioactivity contrasts between granite plutons and metamorphic country rock were smoothed in the heat flow pattern.

To quantify the effect of compositional heterogeneity on heat flow data for the Erzgebirge, we modeled the conductive heat flow along a 100-km-long cross section resembling in a simplified way the upper crustal composition of the Erzgebirge. The 2-D finite element model consists of a 15-km-thick metamorphic basement unit (λ = 3.2 W m^{-1} K^{-1}, A = 2.0 μW m^{-3}) in which a 5-km-thick (square) granite pluton (λ = 3.5 W m^{-1} K^{-1}) of variable heat production (4–12 μW m^{-3}) is emplaced. Heat flow and surface temperature as lower and upper boundary conditions do not vary laterally. The models show that the difference between on-granite and off-granite surface heat flow (Δq_s) increases with increasing difference in radiogenic heat production (ΔA) between the two units and decreases with increasing distance to the heat source contact (Δs). Depending on ΔA, Δq_s is as high as 5–25 mW m^{-2} in close proximity (0–2 km) to a granite intrusion of the size and shape modeled here (D. Stromeyer, personal communication, 1999). This requires us to correct the measured surface heat flow for lateral or vertical heat source effects for many heat flow sites in the Erzgebirge (Table 2).

The model explains the anomalously high surface heat flow observed in the four boreholes (Schönbrunn, Bösenbrunn, Klingenthal, Obergruna), where temperature gradients were measured in metamorphic sequences that are in close proximity (≤1 km) to the underlying Variscan granites of different heat production. Under these conditions the heat flow value measured above the granites must be reduced by ~20 and 7 mW m^{-2}, respectively (Table 2). Surface heat flow reduction of 20 mW m^{-2} is also required for heat flow values determined in the Pobershau and Satzung boreholes in metamorphic rock sequences immediately above the high heat production granites.

Locations affected by lateral heat transfer from a granite heat source are the Zwönitz, Hormersdorf, Riechberg, Großschirma, and Reinsberg boreholes drilled into metamorphic rocks outside the area of granite distribution. However,

Table 2. Correction to Contrasts in Radiogenic Heat Production Applied to Surface Heat Flow[a]

Heat Flow Site	q_s, mW m^{-2}	q_L, mW m^{-2}	q_v, mW m^{-2}	Δs, km	ΔA, μW m^{-3}
Sbr	83		63	<0.3	8
Böu	88		68	<0.2	8
Kt	99		79	<1	8
Tah	112/103[b]				
Zwö	71[b]	66		2	6
Hrm	69[b]	64		2	6
Pob[c]	87/99[b]	92/104			8
Pob[d]	90/92		70/72		8
Szu[c]	89[b]				
Szu[d]	87		67		8
Rieg	70[b]			11	
Grsm	61[b]	60		8	3
Rsb	64[b]	62		3	3
Oba	75		68	1	3

[a]Variables q_s, measured surface heat flow; q_L, surface heat flow corrected for lateral effect of heat source; q_v, surface heat flow corrected for vertical effect of heat source; Δs, distance of heat flow site from the contact; ΔA, contrast in radiogenic heat production.

[b]Values of surface heat flow that are not or only slightly affected by heat flow disturbance from heat production contrasts.

[c]Granite interval.

[d]Metamorphic rock interval.

because of their greater distance from the granite contact, this lateral effect is smaller (1 and 5 mW m^{-2}) than the disturbance in surface heat flow observed in vertical direction.

Finally, the thermal conditions in the granites themselves are affected by radioactivity contrasts. Under the conditions of a large contrast between granites and metamorphic country rocks the higher heat production granite pluton undergoes cooling in close proximity to the contact to the metamorphic rocks, which requires a positive correction of the surface heat flow determined in the granite. This scenario applies to the Pobershau boreholes (see Figure 2) drilled into a granite and located 4 km from the supposed lateral contact with the metamorphic basement. Undisturbed surface heat flow at this site should be higher by 5 mW m^{-2} than the measured one.

7. The q_s-A Plots

A large portion of the surface heat flow from continents is generated within the crust, resulting in a vertical variation in heat flow. Typically, between a few percent and 65% of continental surface heat flow is derived from heat-producing elements in the upper crust [*Rao et al.*, 1982; *Morgan*, 1985]. Traditionally, surface heat flow and radiogenic heat production are used to determine the depth to which the crust is enriched in radioactive elements. *Birch et al.* [1968], *Roy et al.* [1968], and *Lachenbruch* [1968] were the first to describe a linear relationship between q_s and A in plutonic rocks of the same tectonic setting. This linear relationship generally is written in the form

$$q_s = q^* + DA,$$

where q_s is the measured surface heat flow and A is the heat production of the rocks in which the measurement was made. The region where this relationship holds is referred as a heat flow province. The slope of the correlation function (D) is a length scale related to thickness of the crust enriched in radioactive elements. The intercept on the heat flow axis (q^*) is termed the "reduced heat flow." It was originally interpreted as the heat from below the upper crustal heat-producing layer [*Roy et al.*, 1968], consisting of heat generated from radiogenic heat sources in the lower crust and upper lithospheric mantle as well as heat derived from sublithospheric sources [*Morgan and Gosnold*, 1989]. Some subsequent workers [e.g., *Ziagos et al.*, 1985] have identified reduced heat flow with the heat flow in the uppermost mantle. Modern work, however, has demonstrated that this interpretation is likely incorrect [see *Rudnick et al.*, 1998]. The simplest interpretation of this linear relation is that the radioactivity measured at the surface is uniform from the surface to the depth D but varies from place to place, whereas the fraction of heat flow from the lower crust and upper mantle remains uniform within a heat flow province [*Roy et al.*, 1968].

In a first step, a q_s-A plot was constructed that included all measured surface heat flow data, irrespective of whether being disturbed or not (Table 2). This plot yielded a high reduced heat flow (69 mW m^{-2}) coupled with a low D value (3.0 km), which both are geologically and tectonophysically meaningless (see section 8.1). In a second step a q_s-A plot is constructed (Figure 11, curve II) that only takes advantage on q_s data that are not or only slightly affected by heat flow disturbance from heat production contrasts (Table 2). To evaluate the validity of the model on which our corrections of measured q_s values are based, two other plots are calculated. Plot III (Figure 11, curve III) includes, in addition to the data pairs of plot II, q_s values that were corrected for lateral heat flow disturbance (Table 2, q_L). In plot IV, data pairs corrected for vertical heat flow disturbance (Table 2, q_v; not shown in Figure 11 because of overlap with the other lines) were added to the data of plot III. The three q_s-A plots differ only slightly with regard to q^* and D: plot II (measured unaffected q_s): $q^* = 55.6$ mW m^{-2}, $D = 4.6$ km; plot III (II plus corrected q_s, lateral): $q^* = 51.5$ mW m^{-2}, $D = 5.2$ km; and plot IV (III plus corrected q_s, vertical): $q^* = 54.1$ mW m^{-2}, $D = 4.9$ km.

In plots II, III, and IV the A value for each heat flow site represents the weighted average of rocks collected over the depth interval of temperature gradient determination. However, the question arises whether all these values are representative of either the entire granite pluton or the upper crustal metamorphic basement. In the latter case, similarity in heat production and resistance to U leaching poses no serious problems, even if the nature and metamorphic grade of basement rocks change below the depth of heat flow calculation. In the zoned Variscan granites, heat flow sites considered in this study are located in the uppermost and unaltered portions of the hidden plutons, thus minimizing disturbance in heat production resulting from U mobilization. However, drilling has exposed primarily moderately to highly fractionated subintrusions, which are distinguished by the highest A values within a given pluton. Because multiphase plutons typically become more primitive (i.e., less fractionated) with depth, their deeper parts should be characterized by lower heat production. To take these relations into consideration, another q_s-A plot (Figure 11, curve V) is constructed where the heat production values in the granites from Gottesberg, Pobershau, and Satzung refer to values measured in the least fractionated subintrusion exposed by drill core, respectively. This plot yields a lower intercept value with the y axis ($q^* = 45$ mW m^{-2}) and a greater slope ($D = 8.2$ km) compared to plot II, of which it is a modification. These values are considered as minimum for

Table 3a. Crustal Model 1 Used for Heat Budget Calculations Based on Seismic Profiling[a]

Depth, km	Rock Type	V_P, km s^{-1}	ρ, kg m^{-3}	A, μW m^{-3}
5–8	Variscan granite	5.5–5.9	2.66	5.6–11.6
15	parametamorphic and orthometamorphic upper crust[b]	5.9–6.3	2.78	2.2
23	mafic amphibolite/felsic gneiss	6.3–6.6	2.88	1.0[c]
30	metabasite/mafic granulite	6.8–7.2	3.05	0.3[d]

[a]From *Behr et al.* [1994]. Note that for calculation of the mantle heat flow, model 1 was modified in such a way that the entire upper crust to a depth of 15 is composed of parametamorphic and orthometamorphic upper crustal rocks only. Radiogenic heat production rates for upper crustal rocks are from this study.
[b]Including phyllite, mica schist, paragneiss, metagranite/metagranodiorite, migmatite.
[c]Average heat production of the middle continental crust [*Rudnick and Fountain*, 1995].
[d]Average heat production of the lower continental crust in Paleozoic orogens [*Rudnick and Fountain*, 1995].

q^* and maximum for D in the Erzgebirge derived from the q_s-A plots.

8. Discussion

8.1. Reexamination of the Surface Heat Flow/Heat Production Relationship

The curves in Figure 11 define rather high q^* values, ranging from 45 to 52 mW m^{-2}. According to traditional q_s-A plot interpretation and the observation that the portion of the crust below an enriched crustal layer is typically depleted in radioactive elements, this high reduced heat flow would be also an indication for an anomalously high mantle heat flow. The D values determined for the Erzgebirge (4.6–8.2 km) differ from the thicknesses of the enriched crust deduced from the Armorican massif (15.6 km [*Jolivet et al.*, 1989]) and from SW England (16.6 km [*Lee et al.*, 1987]), which are regarded as representing typical Variscan crust in Europe. However, they are well within the range of thicknesses of Erzgebirge granite plutons estimated from seismic profiles (3–10 km [*Behr et al.*, 1994]) and 3-D gravity modeling (5–13 km [*Choi*, 2000]). Furthermore, the D values of the Erzgebirge concur with the depth of root zones of Variscan granites from the neighboring Fichtelgebirge (see Figure 1) (6–8 km [*Vigneresse*, 1999]) and global estimates of the thickness of peraluminous granite plutons emplaced in the upper parts of the Earth's crust (7 ± 2 km [*Vigneresse*, 1988]).

These observations give rise to two basic questions when interpreting the q_s-A plots for the Erzgebirge: (1) Is there independent evidence for a high reduced heat flow and, hence, mantle heat flow beneath the area? (2) Are the D values compatible with the thickness of the crust enriched in heat-producing elements?

To answer these questions, straightforward 1-D heat balance calculations are made for Erzgebirge crustal models that vary in structure and composition. Two general cases are distinguished for each model: (1) upper crust where Variscan granites are absent (area of off-granite heat flow sites) and (2) upper crust containing granites (area of on-granite heat flow sites). The first structural model calculated (hereafter referred as model 1) is derived from deep seismic soundings [*Behr et al.*, 1994] and describes the Erzgebirge crust as being composed of a thick and felsic upper crust (15 km) of metagranitic to granodioritic composition and diverse parametamorphic rocks (Table 3a). In the area where Variscan granites occur (case 2), they make up the uppermost part of this 15-km layer with an average thickness of 5 km. The V_P patterns are consistent with a thin and relatively felsic middle crust (15–23 km), which is interpreted as a mixture of mafic amphibolites and felsic gneisses. The lower crust is also thin (7 km) and is assumed to be composed mostly of mafic granulites. The total crustal thickness is set to 30 km (range of Moho depth beneath the Erzgebirge 28–32 km [*Behr et al.*, 1994]). The second structure model (hereinafter referred as model 2) is based on gravimetric data and gravity modeling [*Choi et al.*, 1998; *Choi*, 2000]. In this model (case 1) the upper crustal layer is considered as being thinner (13 km) and underlain by a 7-km-thick layer of intermediate pyroxene granulites above a 10-km-thick layer composed mostly of mafic granulites (Table 3b). In case 2 the upper crust is divided into an upper 5-km-thick layer of Variscan granites underlain by the undepleted metamorphic basement.

Heat production values for granites and upper crustal metamorphic rocks are from this study (see section 5). Explicitly, the heat production values for the upper crustal metamorphic layer (2.2 μW m^{-3}) refer to the lower end of range of heat production in these rocks measured on surface or near-surface samples. In this layer, significant variation of heat production with depth is unlikely, following observations from deep bore-

Table 3b. Crustal Model 2 Based on Gravity Modeling[a]

Depth, km	Rock Type	V_P, km s^{-1}	ρ, kg m^{-3}	A, μW m^{-3}
5–8	Variscan granite	5.6–5.9	2.62	5.6–11.6
10	parametamorphic and orthometamorphic upper crust[b]	5.9–6.1	2.76	2.2
20	intermediate (pyroxene) granulite	6.1–6.5	2.83	0.3[c]
30	mafic granulite	6.6–7.2	2.9–3.0	0.2[c]

[a]From *Choi* [2000]. Note that for calculation of the mantle heat flow, model 2 was modified in such a way that the entire upper crust to a depth of 10 km is composed of parametamorphic and orthometamorphic upper crustal rocks only.
[b]Including phyllite, mica schist, paragneiss, metagranite/metagranodiorite, migmatite.
[c]Heat production of granulites from the Granulitmassiv [*Müller et al.*, 1987].

holes [*Arshavsakaya et al.*, 1987; *Clauser et al.*, 1997]. Well-constrained global averages of radiogenic heat production [*Rudnick and Fountain*, 1995] were taken as representative values for the middle and lower crust in model 1 (see Table 3a) because little direct evidence is provided from rare enclaves in Tertiary basalts of the Erzgebirge to determine the composition of these units. Following the structural concept of *Choi et al.* [1998] and *Choi* [2000], U-Th-K data of unaltered intermediate pyroxene granulites and mafic granulites from the neighboring Granulitmassiv [*Müller et al.*, 1987] are used to calculate A values that are suggested to be typical for the middle and lower crust in model 2. In all calculations a step model of radiogenic heat production distribution was considered because it is a better approach to the layered nature of the Erzgebirge crust with its strong contrasts in radiogenic heat production than are linear or exponential functions of radioactivity in plutonic rock discussed by *Lachenbruch* [1970].

To understand the geological significance of the high reduced heat flow derived from the q_s-A plots, it is appropriate to exclude the effects of heterogeneity in the radiogenic heat production in the upper crust. This is accomplished by considering data from off-granite heat flow sites (case 1), where the five corrected q_s values average to 63 mW m^{-2}. In model 1, surface heat flow of 63 mW m^{-2} is reproduced if the heat flow at the crust-mantle boundary is set to 20 mW m^{-2}. What is termed reduced heat flow, here is the heat flow at 15 km depth. It amounts to 30 mW m^{-2} so that 10 mW m^{-2} of heat flow is attributed to heat sources in the deep crust. The 33 mW m^{-2} accounted for by the 15-km-thick upper crust amounts to 77%, and the 15-km-thick middle/lower crust to 23% of the entire crustal heat flow (43 mW m^{-2}; 68% of the surface heat flow). To fit the surface heat flow of 63 mW m^{-2} in model 2, a significantly higher mantle heat flow of 30 mW m^{-2} is required. Here, the proportion of total crustal heat flow budget generated in the upper 10 km is 87% (29 mW/m^2) and that in the deeper depleted layers is 13% (4 mW m^{-2}). The reduced heat flow, here at 10 km depth, yields 41 mW m^{-2}. The heat flow through the Moho derived from model 1 is slightly lower, whereas that from model 2 is slightly higher than the estimate for the Bohemian massif, of which the Erzgebirge is part (26 mW m^{-2} [*Čermák*, 1989]).

To account for the on-granite surface heat flow between 90 and 110 mW m^{-2}, the 5-km-thick layer of Variscan granites (case 2 in both models 1 and 2) must generate an additional heat flow between 38 and 58 mW m^{-2}. Hence the uppermost, thin part of the crust composed of HHP granites produces almost half (40–50%) of the surface heat flow in Erzgebirge granite areas. The contribution of crust to surface heat flow amounts to 70–80% (70–90 mW m^{-2}, model 1; 64–84 mW m^{-2}, model 2). Heat production rates between 7.6 and 11.6 μW m^{-3} are required to fit the observed range in surface heat flow. For a granite thickness of 8 km (see section 7) the heat production rates are correspondingly lower (5.6–8.1 μW m^{-3}). Nevertheless, they all fit well in the range of heat production measured in unaltered granite samples at or close to the surface. Granite plutons of less thickness or lower radiogenic heat production, as represented by most type 1 and type 2 granites, should give rise to lower surface heat flow, but unfortunately, no boreholes and hence heat flow determinations are available to test this speculation.

Results of heat budget calculations have shown that the reduced heat flow determined from the Erzgebirge q_s-A plots is irreconcilable with its initial interpretation as measure of heat from below the crustal layer enriched in heat-producing elements. Clearly, the q^* value also has nothing in common with the heat flow at the crust-mantle boundary. In fact, it is identical with the heat flow at the base of the HHP granite layer within the upper crust (52 and 45 mW m^{-2} for granite thicknesses of 5 and 8 km) and does not represent the heat flow in the middle crust as suggested by *Furlong and Chapman* [1987].

8.2. Variation of Radiogenic Heat Production in Granitic Rocks: Further Implications for the q_s-A Linear Relationship

The geothermal study of the Erzgebirge underscores the complications involved in determining representative heat production values for a single heat flow site. Given the strong dependence of the degree of fractionation of igneous rocks on the concentration of heat-producing elements, heat production data obtained at the depth interval where the temperature measurements are performed will rarely reflect the average radiogenic heat production in a multiphase pluton, where U and Th in particular, are zoned. If the borehole has penetrated less fractionated subintrusions, which are usually located in deeper and marginal parts of a pluton, the average heat production is underestimated, giving rise to an overestimation of the thickness of the granite layer and an underestimation of reduced heat flow below this layer. On the other hand, if highly fractionated granites preferentially are encountered in the borehole, the average heat production is overestimated, and consequently, lower D and higher q^* values will be obtained from the q_s-A plot. In the granite plutons discussed here, spatial variations of the radioactive elements in unaltered samples are systematic and result from magma differentiation by fractional crystallization [*Förster et al.*, 1999]. They are not related to a combined migration-diffusion process in the fluid phase during and after solidification of the melts, a process that has been invoked by *Rybach and Buntebarth* [1981] as important in controlling the abundance and distribution of the HHP elements in granitic magmas.

In the Erzgebirge, leaching and redistribution of U is associated with the circulation of meteoric water long after solidification of its host granites [*Förster et al.*, 1998]. The reduced nature of the residual fluids released from the crystallizing magmas [*Förster and Tischendorf*, 1989] precludes them carrying significant amounts of U while invading the surrounding rocks. Uranium can only be mobilized and transported over greater distances in highly oxidizing solutions [*Dubessy et al.*, 1987]. Thus magmatic fluid-triggered migration of U within the granite itself or into its surroundings, as discussed by *Rybach and Buntebarth* [1981], requires distinct physicochemical conditions and is far from being of universal significance.

Where heat flow sites occur in altered portions of a granite body, leaching of uranium, which is the main contributor to rock radioactivity, may significantly lower the radiogenic heat production, thus overestimating D and underestimating q^*. The same effect may occur when heat production from surface granite samples is combined with heat flow data determined in boreholes exposing unaltered granites. The utilization of A values from altered samples for q_s-A plot construction is valid only when the bulk of U is fixed in accessory minerals that are relatively resistant to alteration (monazite, xenotime, zircon, Th-rich uraninite). Heat flow studies in granites containing easily leachable Th-poor uraninite must be restricted to fresh rock samples.

Table 3c. Crustal Model 3[a]

Depth, km	Rock Type	V_P, km s^{-1}	ρ, kg m^{-3}	A, μW m^{-3}
5	Variscan granite	5.6–5.9	2.62	6–12
13	parametamorphic and orthometamorphic upper crust[b]	5.9–6.1	2.76	2.2
20	60% felsic and 40% intermediate granulite	6.3–6.6	2.88	0.8[c]
30	50% mafic granulite, 25% intermediate granulite, 25% felsic granulite	6.8–7.2	3.05	0.5[c]

[a]Interpretation of the seismic velocity (V_P) and density (ρ) data for the middle and lower crust in terms of their average compositions in Paleozoic orogens. See *Rudnick and Fountain* [1995].
[b]Including phyllite, mica schist, paragneiss, metagranite/metagranodiorite, migmatite.
[c]Calculated on the basis of the median A values for felsic, intermediate, and mafic granulites in post-Archean terrains reported by *Rudnick and Fountain* [1995].

8.3. Nature and Composition of the Depleted Crust

Crustal models 1 and 2 differ in composition of the middle and lower crust (see Tables 3a and 3b). Information on these layers is essential to calculate the mantle heat flow beneath the Erzgebirge. Unfortunately, from surface observation the distribution of heat sources in the deep continental crust can barely be identified. However, in view of the large masses and the evolved nature of the granites the thick unit of middle and lower crust in model 2 is too mafic (and thus too low in U and Th) to constitute the restites left behind after granite melting. Under the assumption that the present 30-km-thick crust represents the source region of these granites, model 2 has to be discarded, which also implies that mantle heat flow of 30 mW m^{-2} is an overestimate for the Erzgebirge.

Furthermore, the P wave seismic velocities measured in the Erzgebirge crust can easily be explained in terms of lithologies other than those considered by *Behr et al.* [1994] and *Choi* [2000]. In crustal model 3 (Table 3c), which is a modification of model 1, we have interpreted the P wave velocities and densities of the middle and lower crust in terms of rock types usually observed in European Paleozoic orogens [*Rudnick and Fountain*, 1995]. With a mantle heat flow of 21 mW m^{-2} this crustal profile (with A values calculated from averages for the individual rocks provided by *Rudnick and Fountain* [1995]) perfectly satisfies the surface heat flow in the Erzgebirge.

Moreover, recent geochemical studies of high-grade orthometamorphic and parametamorphic rocks imply that the difference in heat production between a granulite-facies rock and its amphibolitic counterpart is typically <0.3 μW m^{-3} [*Hansen et al.*, 1995; *Bingen et al.*, 1996; *Bea and Montero*, 1999]; a difference too small to distinguish from surface heat flow measurements. Therefore amphibolite-facies rocks may constitute part or most of the middle and lower crust in the Erzgebirge, in much the same way as parametamorphic formations (metagraywackes and metapelites) may accompany, in minor amounts, the granulite-facies metaigneous rocks considered in our heat budget estimations.

8.4. Conductive Mantle Heat Flow Below the Erzgebirge

The off-granite surface heat flow in the Erzgebirge is significantly higher than that in Archean regions (~42 ± 12 mW m^{-2} [*Pinet et al.*, 1991; *Nyblade and Pollack*, 1993; *Jaupart and Mareschal*, 1999]) and is at the upper end of nonorogenic heat flow in Proterozoic regions far removed from Archean cratons (55 ± 17 mW m^{-2} [*Nyblade and Pollack*, 1993]). These averages differ from previous estimates (e.g., 65 ± 1.6 mW m^{-2} [*Pollack et al.*, 1993]), which have considerably overestimated the average heat flow in thermally stable continents. Recent estimates of mantle heat flow in nonorogenic terrains are numerous and generally range from 9 to 17 mW m^{-2}, with most values being of the order of 10–13 mW m^{-2} [*Pinet et al.*, 1991; *Frottier et al.*, 1995; *McLennan and Taylor*, 1996; *Mareschal et al.*, 1999]. They do not support previous calculations yielding uniform mantle heat flows as high as 27–28 mW m^{-2} [*Vitorello and Pollack*, 1980; *Morgan*, 1984] and corroborate the idea that the average mantle heat flow is almost independent of crustal age [*Jaupart and Mareschal*, 1999].

Compared to these most recent results, mantle heat flow in the Erzgebirge (20–30 mW m^{-2}) is slightly to modestly higher than that in thermotectonic stable areas. Mantle heat flow usually can be elevated owing to (1) transient heat associated with preceding tectonothermal activity, (2) heat expelled from an active magma chamber, or (3) heat generated from a metasomatically enriched upper mantle.

The major crustal consolidation of the region occurred in late Carboniferous/early Permian time. Taking this and the thermal relaxation time constant of the lithosphere (100–200 Ma [*Lachenbruch and Sass*, 1977; *Morgan*, 1984]) into account, thermal transients from tectonothermal events related to the Variscan orogeny can be excluded.

However, southeast of the Erzgebirge fault, crustal stresses associated with the Alpine-Carpathian orogeny caused tectonic reactivation of old tectonic sutures, which resulted in creation of the Ohře (Eger) rift (see Figure 1). This rift zone is site of ultramafic and more differentiated volcanism that took place from the late Cretaceaous to Quaternary (~79 to 0.26 Ma). These rocks, as well as mantle xenoliths in Tertiary basalts, are remarkably enriched in U, Th, and other incompatible elements. Although inferring heat production of the lithospheric mantle from xenoliths is difficult [*McDonough*, 1990; *Rudnick et al.*, 1998], available compositional data are interpreted in terms of a metasomatically enriched mantle beneath the rift [*Ulrych and Pivec*, 1997]. Furthermore, seismic profiling [e.g., *Tomek et al.*, 1997] as well as gas studies [*Polyak et al.*, 1985; *Weinlich et al.*, 1999] corroborate the idea of an active and likely basaltic magma chamber in the upper mantle below the intracontinental rift. Thus the high surface heat flow in that rift, locally approaching 90–100 mW m^{-2} in granite areas, is thought, although not yet convincingly proven, to be generated by mass flow from the hot mantle during Alpine activation of the Bohemian massif, a view that has also been adopted for the thermal regime in the Erzgebirge [*Polyak et al.*, 1985]. Indeed, magma in the upper mantle of the rift zone may have an impact by lateral heat conduction on the mantle heat flow beneath the adjacent Erzgebirge. Alternatively, the mantle below the Erzgebirge may contain elevated abundances of heat-

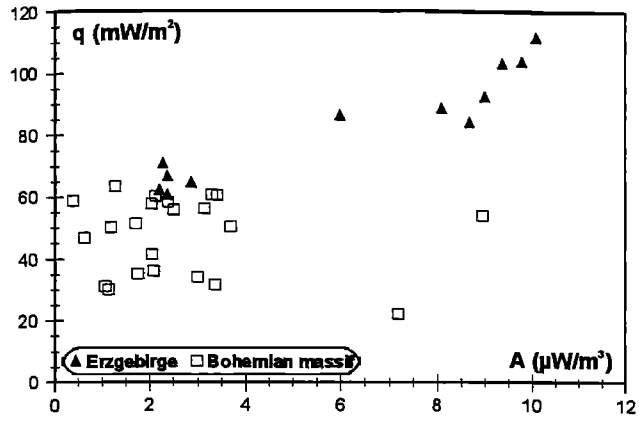

Figure 12. Summary of q_s-A data for the Bohemian massif. Data from the German Erzgebirge are plotted separately from those for the remaining parts of the massif (data from *Ostřihanský* [1980] and *Čermák* [1981]).

producing elements. Enrichment in Th, U, and K is suggested as a typical feature of the European Cenozoic subcontinental mantle [*Dunai and Baur*, 1995] implying that all of central Europe should have an elevated mantle heat flow, as shown by *Čermák* [1993]. However, most values used to construct the European Moho heat flow pattern are derived from q_s-A relations and therefore must not be necessarily true, as shown in this paper. Irrespective of the cause of the higher mantle heat flow below the study region, it is a minor component of the surface heat flow relative to the effects of Variscan granites.

8.5. Bohemian Massif: A Single Heat Flow Province?

Variation of surface heat flow in the study area is shown to be entirely attributed to heterogeneities within the crust. Mantle heat flow in off- and on-granite areas is likely the same, enforcing characterization of the Erzgebirge as one heat flow province.

Figure 12 summarizes published q_s-A data for the Bohemian massif, which display a broad scatter and, in contrast to what is observed in the Erzgebirge, do not follow a straight line. Part of this scatter can be related to crustal heterogeneity within the massif, which is a collage of nine structurally and genetically distinct units [see *Ostřihanský*, 1980]. However, surface heat flows of 40 mW m^{-2} and lower in parts of the massif are irreconcilable with the increased mantle heat flow below the Erzgebirge. Therefore the massif cannot be regarded as a single heat flow province as suggested by *Ostřihanský* [1980] and *Čermák* [1981], and previous attempts to construct a q_s-A plot for the entire massif [*Čermák*, 1975a, 1981] are geologically unjustified.

8.6. Different q_s-A Plots for European Variscan Provinces: Real or Coincidental?

The q_s-A plots constructed for SW England (Cornubian batholith) and western France (Armorican massif) determine reduced heat flows of 27.0 and 26.6 mW m^{-2} and thicknesses of the enriched upper crust of 16.6 and 15.6 km for both Variscan provinces [*Lee et al.*, 1984; *Jolivet et al.*, 1989]. Their crustal structure and composition is similar to the Erzgebirge. Therefore the question arises as to why the q_s-A plots for SW England and western France correlate well with the crustal geology and the Erzgebirge plot does not. Reevaluation of the fundamental data on which the q_s-A plots for SW England and western France are based reveals some inconsistencies in the data, suggesting that the q^* and D results are coincidental.

In SW England, which is part of the Rhenohercynian zone of the Variscan belt, concentration of heat-producing elements for the Cornubian granites was apparently measured exclusively on surface samples. Most granites are geochemically and mineralogically similar to granites forming the high-F, high-P_2O_5 group in the Erzgebirge and also contain easily leachable Th-poor uraninite as the main carrier of U [*Basham et al.*, 1982; *Webb et al.*, 1985]. Comparison of the U-Th systematics in surface Cornubian granites and not exposed Erzgebirge granites of the same type supports previous suggestions [*Webb et al.*, 1985] that many Cornubian samples experienced significant U depletion. Thus underestimation of heat production in the SW England granites might be on the same order of magnitude as that produced if one used data from U-depleted surface samples from the Eibenstock pluton for calculating the radiogenic heat production in the Erzgebirge granite layer. Furthermore, for the original q_s-A plot, data from Cornubia were combined with data from metamorphic basement rocks in central England and Wales. Yet reevaluation of heat flow data from the United Kingdom [*Webb et al.*, 1987] suggests that southern Britain does not form a single thermal province, as proposed by *Lee et al.* [1987]. In summary, both factors may explain the greater D and lower q^* of the SW England q_s-A plot relative to the Erzgebirge plot.

The q_s-A plot for the Armorican massif in western France might suffer from another problem. We cannot reproduce the A values published by *Vigneresse et al.* [1989] from the U-Th-K_2O contents listed in their Table 1. Actually, heat production in these rocks is between 1.5 and 2.5 times higher than they give. Using the recalculated A values significantly decreases D and increases q^*, thus better approaching the relations observed in the Erzgebirge. Unfortunately, it is not possible to determine from *Jolivet et al.* [1989] whether the incorrect A values given by *Vigneresse et al.* [1989] were used in the resultant q_s-A plot for western France. Therefore evaluation of validity of that plot remains speculative.

9. Summary and Conclusions

The combined heat flow/heat production study of the German Erzgebirge allows a number of conclusions to be drawn of both regional and general significance.

9.1. Regional Significance

1. The Erzgebirge crust is enriched in radioactive elements to a depth of ~15 km; beneath this depth the crust is composed mostly of rocks depleted in radiogenic elements. The middle and lower crust probably consists of felsic, intermediate, and mafic amphibolites or granulites in various proportions. Detailed interferences on their nature and compositions, however, cannot be made from surface heat flow patterns.

2. The crustal model derived from deep seismic sounding [*Behr et al.*, 1994] is in better agreement with the thermal and compositional data than is the model developed from gravimetric modeling [*Choi*, 2000]. Low surface heat flow values in off-granite areas (27–39 mW m^{-2}) reported by *Hurtig and Oelsner* [1979] are not confirmed by heat conduction and are irreconcilable with any plausible composition of the crust.

3. The surface heat flow patterns are consistent with a slightly enhanced mantle heat flow of the order of 20–30 mW m^{-2}. Petrological constraints support a mantle heat flow that is

likely at the lower end of that range. Therefore, in the Erzgebirge, 5–10 mW m^{-2} of heat flow are likely supplied from the mantle in excess to average mantle heat flow observed in tectonically stable terrains.

4. Elevated surface heat flows (90–110 mW m^{-2}) occur in Variscan granites, which are on average between 5 and 8 km thick and account for 40–50% of the measured values. High surface heat flows are not related to an abnormally high conductive mantle heat flow [*Čermák*, 1975b, 1989] or to heat advection from regional or local fluid flow along deep-seated fault systems, as previously suggested [*Polyak et al.*, 1985; *Hurtig and Oelsner*, 1979].

5. Heat production of the Erzgebirge crust (1.4 μW m^{-3} in off-granite regions and up to 3 μW m^{-3} in areas of granite occurrence according to model 1) is significantly higher than that calculated from global estimates of the bulk composition of the continental crust, ranging from 1.31 [*Shaw et al.*, 1986] to 0.58 μW m^{-3} [*Taylor and McLennan*, 1985]. High crustal heat production is primarily related to the upper, 15-km-thick crustal layer, ranging from 2.2 μW m^{-3} in off-granite regions to 6.7 μW m^{-3} in areas of highest heat flow in granites, which is ~4 times higher than the average heat production in the Earth's upper continental crust (1.8 μW m^{-3} [*Taylor and McLennan*, 1985]). Where granites occur, the crust contributes, on average, 70–90 mW m^{-2} to the surface heat flow, which is some 2–4 times higher than would be expected from the estimates of the average composition of the continental bulk crust.

9.2. General Significance

1. When significant heterogeneities in crustal heat production exist, inferences from q_s-A plots about the thermal structure of the crust and the heat flow through the Moho are suspect and must be viewed with caution. The reduced heat flow value reflects heat flow at the base of the HHP granites and not the one below the crust enriched in radiogenic elements, as proposed in earlier works. Therefore, in a number of heat flow studies worldwide the amount of high mantle heat flow or transient heat flow may be significantly overestimated. The "thermal depth" is a measure of the average thickness of the granites and does not correspond properly to the depth to the depleted granulite layer as invoked by *Vigneresse* [1990]. In the situation of the Erzgebirge, that depth is underestimated by 30–50% [see also *Vigneresse and Cuney*, 1991]. The depth to the depleted parts of the crust is probably only portrayed correctly in a q_s-A plot when the upper crust is fairly uniform in heat production.

2. Evaluation of heat flow disturbances demonstrates that heat conduction (lateral or vertical) from a strong heat source in the upper crust has an enormous impact on the measured surface heat flow. However, even if all q_s values are corrected accordingly, neither the thickness of enriched crust nor the rate of reduced heat flow is correctly portrayed in the q_s-A plot.

3. For heat flow sites in multiphase, compositionally zoned granitic plutons, determination of "representative" radiogenic heat production values suffers from heterogeneous vertical and horizontal distribution of radioactive elements. Within such a pluton, heat production in highly fractionated granites could exceed 5 times or more the heat production measured in less fractionated granites.

4. Mass balance calculations define U and Th as major contributors to rock heat production. Uranium is by far the most critical component, given its considerably higher susceptibility to leaching relative to Th. Thus surface samples may show A values that are up to 5 times lower than those of subsurface samples from the same granite. Regional U depletion in granites may reach depths of several kilometers beneath the surface. Peraluminous granites containing Th-poor uraninite are particularly susceptible to U depletion and thus are problematic objects for heat flow studies. However, in a global view the vertical distribution of heat sources within the enriched crustal layer seems primarily controlled by magmatic and metamorphic processes rather than by alteration processes involving crustal fluids, as invoked by *Čermák and Rybach* [1989]. Notwithstanding, element redistribution processes due to fluid-rock interaction may be locally or even regionally significant.

5. To minimize chance for incorrect interpretation of q^* and D values, q_s-A plot construction should be performed in concert with heat budget calculations. This, of course, requires that both structure and composition of the crustal segment are well documented by geophysical and geochemical data.

Appendix A: Analysis of Temperature Profiles

Temperatures were obtained with analog-reading thermistor probes. The accuracy of the measurements was ±1°C [see *Fricke and Schlosser*, 1980]. However, it is likely that during the 15-year period of using different thermistor tools, calibration errors occurred that affect the absolute temperatures but not the overall geothermal gradient. For most boreholes a temperature-depth profile was available, where temperature is plotted in 50-m intervals as read from the original log. In a few instances, the original and detailed temperature profile was recorded at smaller logging intervals, which was then digitized.

Generally, main factors perturbing temperatures in a 1-D heat conduction setting are terrain, microclimatic effects, fluid flow, and inhomogeneous thermal conductivity [*Blackwell and Spafford*, 1987]. The topography in the study area is relatively subdued because of the extensive erosion since the Paleozoic, so that morphologic features in the vicinity of the boreholes are either negligible or of the order of few tens of meters. To exclude these small terrain effects and near-surface microclimate changes, all temperature logs used in this study (Figures A1–A4) were plotted and interpreted at depths >100 m, which also is below the watertable. At these depths, all boreholes were open. Several wells were not accessible to total drilling depth at the time the temperature log was obtained.

The temperature logs obtained at the Schönbrunn (Sbr) site (Figure A1a) reflect the different hydraulic properties in the subsurface as they were reported by *Kuschka and Hahn* [1996] for the entire Schönbrunn (Sbr)/Bösenbrunn (Böu) mining district in the SW Erzgebirge. Tectonically undeformed units of metamorphic bedrock of low hydraulic transmissivity T_v = 10^{-6}–10^{-9} m^2 s^{-1}, in which heat transfer is by diffusion, are intersected with main faults, where rock mylonitization is responsible for a high rock transmissivity of the order of T_v = 10^{-3}–10^{-1} m^2 s^{-1}. The loss of drill mud during exploration drilling indicates that these zones of high hydraulic conductivity occur at depths between 100 and 800 m. In addition, because of the mining activities, bedrock has become increasingly depressed so that fracture porosity and permeability have increased steadily in conjunction with an increased fluid release during the dewatering of the mining field. The depression cone in the mine has activated an upward flow of thermal water. As a consequence of these conditions, several logs (Sbr 7, Sbr 8,

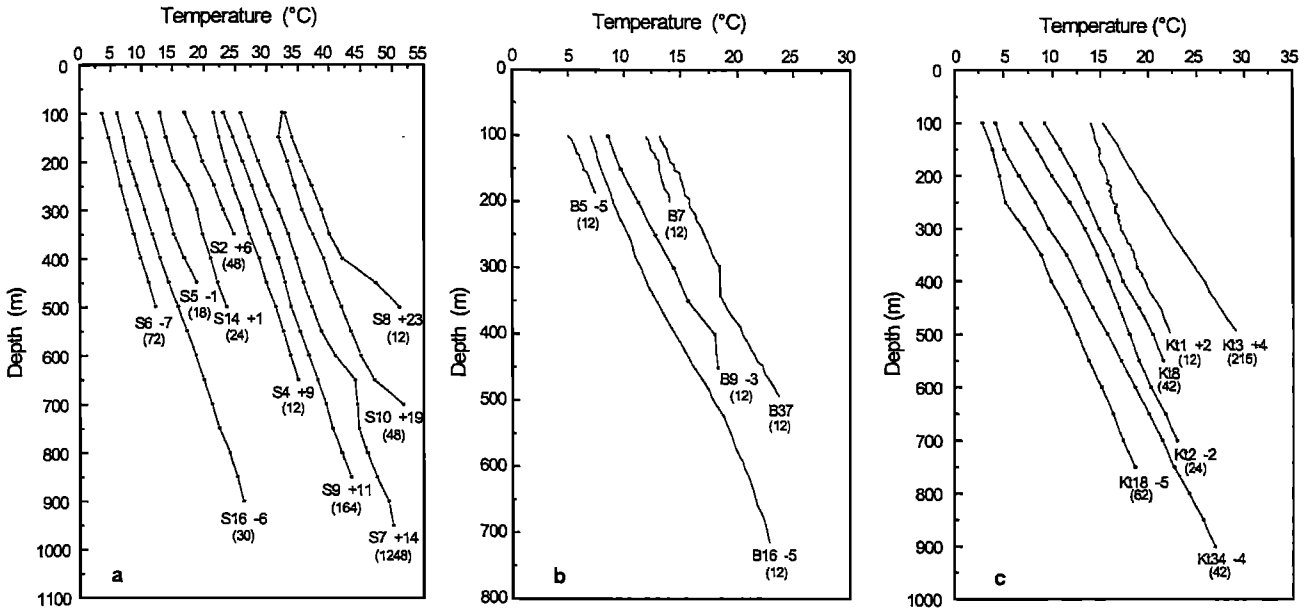

Figure A1. Temperature-depth curves for boreholes in (a) the Schönbrunn area (Sbr), (b) the Bösenbrunn area (Böu), and (c) in the Klingenthal area (Kt). Temperature logs digitized from an original hardcopy are shown as single line, temperatures-depth profiles obtained from a hardcopy in 50-m depth intervals as stippled line. To avoid overlap, the curves are offset from origin by different increments (°C) given behind log ID, e.g., −7. The shut-in time in hours is given in parentheses below log ID. The log ID "S" and "B" stand for Sbr and Böu, respectively. Small-scale irregularities in the character of the digitized logs are evidence for local disturbances caused by fluids shortly after cessation of drilling.

and Sbr 10) show distinctive effects of fluid flow perturbations. The intervals of perturbations are coincident with the depth intervals where the boreholes intersect the main thrust fault of the deposit where regional upward flow of thermal waters is proposed. Several logs, for example, the Sbr 6 log, were too shallow to record the inflow of thermal water that might occur in the bottom part of the well. However, the logs also show that several depth intervals are not affected by dynamic conditions.

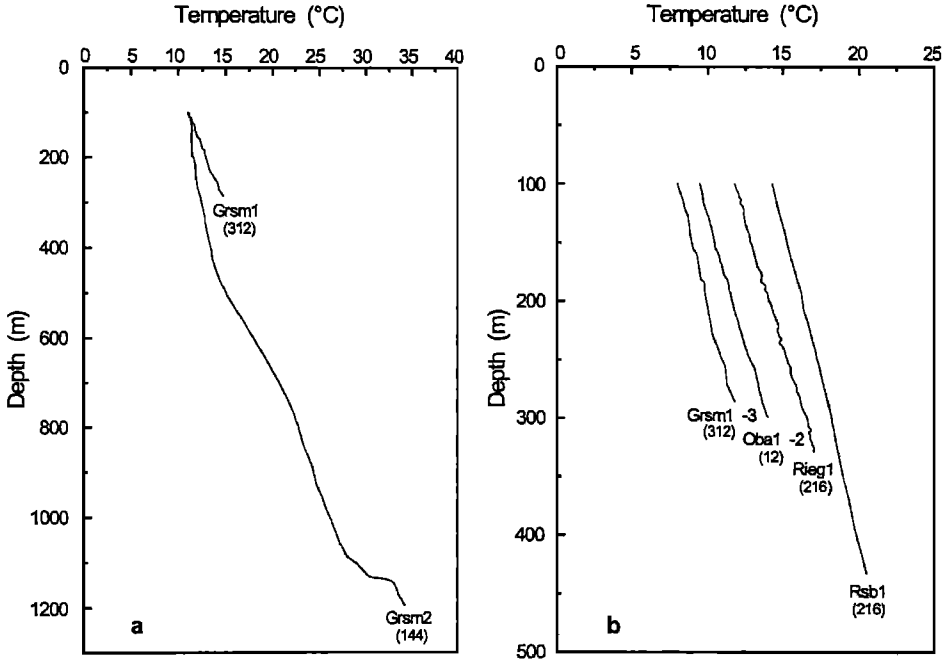

Figure A2. Temperature-depth curves for (a) the deep and shallow Grsm boreholes and (b) the boreholes Grsm 1, Oba 1, Rieg 1, and Rsb 1 near Freiberg, in the eastern part of the Erzgebirge. Shut-in time in hours in parentheses. The Grsm 1 and Oba 1 temperature logs are offset from origin by −3°C and −2°C, respectively.

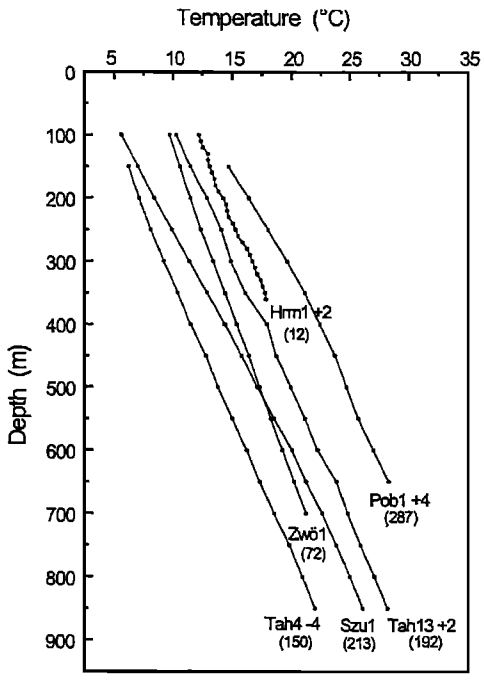

Figure A3. Temperature-depth curves from the Tah 4 and Tah 13 boreholes and the Szu 1 and Pob 1 boreholes bottomed into granite plutons in comparison with the Zwö 1 and Hrm 1 boreholes penetrating phyllites and schists. Offset of temperatures from origin is given behind log ID. Shut-in time is given in parentheses.

Sbr 2, 4, 5, and 16 boreholes have more or less linear temperature-depth profiles because of their location on the flanks of the fluorite deposit structure where the wells penetrate the units of low-permeability rocks. Figure A1b shows comparable features observed in the temperature-depth profiles of the Bösenbrunn (Böu) deposit. The boreholes are located approximately on a line 1.5 km in length, with a distance between each borehole of ~250 m. Subsurface thermal conditions partly affected by active water flow are seen in the logs Böu 9 and Böu 37. Also the thermal conditions in the shallow Böu 7 hole may be a reflection of fluid flow. This is indicated by the low gradient compared to the other logs and an inferred surface temperature T_0, which is higher as the annual ambient temperature of 7–8°C for the area [*Diener et al.*, 1984]. Tool calibration may be the reason for some of the offset in the remaining temperature logs. Availability of a suite of logs at the Sbr and Böu sites makes it possible to select for heat flow determination those depth intervals that are under heat conduction conditions.

In the Klingenthal (Kt) area, temperature logs are available from six boreholes (Figure A1c), which are in close proximity. The wells are ~2.5 km apart (boreholes Kt 1, Kt 2, and Kt 3) and about 5.5 km south of boreholes Kt 8, Kt 18, and Kt 34; the latter are located on a line ~1.7 km in length. Although phyllite and mica schist encountered by the boreholes are highly impermeable in general, fluid flow occurs in zones of intensive fracturing (mylonitization) and faulting. For example, whereas the Kt 18 log is affected only by local flow in the upper part of the hole, the entire Kt 1 log shows the typical sign of upward water flow reflecting a low temperature gradient and a surface temperature T_0 of 11°C that is higher than the mean annual temperature of 4–5°C reported for this area of higher altitude. Although measured 216 hours after last drill mud circulation, the high 34.8°C km^{-1} gradient observed in the Kt 3 hole also may not reflect the overall heat flow conditions typical for the site. Again, this is indicated by a too high surface temperature T_0 of 7.7°C.

Another situation of substantial perturbations of temperature is the borehole Grsm 2 (locality Großschirma), where the temperature log measured after a shut-in time of 144 hours shows distinctive curvatures (Figures A2a). Stabilized intraborehole flow in several depth intervals is proposed as the thermal conductivity of the rock types (gneiss and granite) encountered cannot account for the gradient differences observed. Therefore the temperature gradient for heat flow calculation was determined from the temperature profile measured in the nearby shallower Grsm 1 borehole, where the temperature gradient is quasi-identical with the gradient observed near the bottom of the Grsm 2 well, which is below the fluid-affected depth interval.

The logs in Figure A2b are representative for heat conduction conditions as are the logs for large depth intervals in Figure A3. The determination of a reliable heat flow value requires that the borehole is at thermal equilibrium when the temperature measurements are made. Typically, in deep wells, temperatures that have cooled down during drill mud circulation in the near-bottom part return to equilibrium relatively fast in contrast to the heated uppermost part of the well, which adjusts more slowly. This effect is more prominent the deeper the well. Therefore the deviation of the uppermost part of the temperature profile from the surface (ground) temperature is a good estimate whether thermal conditions in the borehole are attained. To develop a correction factor for disturbed Erzgebirge temperature profiles, the Horner plot method was

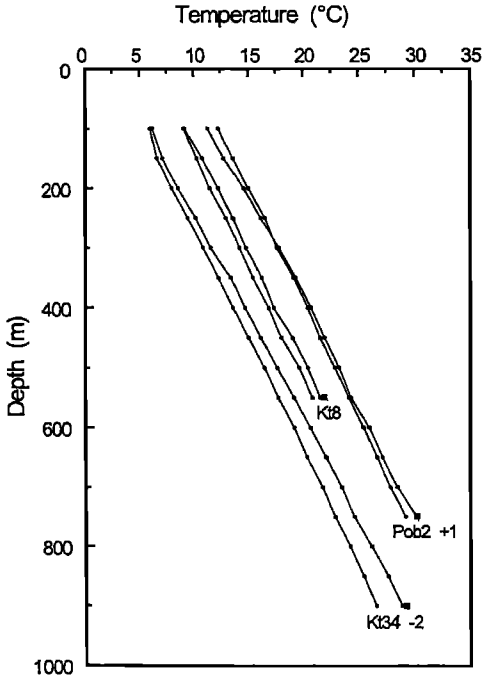

Figure A4. Repeated temperature logs in the Pob 2, Kt 8, and Kt 34 boreholes with the 'equilibrium' bottom-hole temperature value (solid square) determined using the Horner method. The shut-in times are 7 and 240 hours (Pob 2), 12 and 42 hours (Kt 8), and 4 and 42 hours (Kt 34). Offset of each temperature log pair from origin is given behind log ID.

Table A1. Thermal Conductivity Measured on Dry Rock Samples From Major Rock Types[a]

Rock Type	λ_e Range, W m^{-1} K^{-1}	λ_e Mean ± S.D., W m^{-1} K^{-1}	λ_{II} Range, W m^{-1} K^{-1}	λ_{II} Mean ± S.D., W m^{-1} K^{-1}	λ_z Range, W m^{-1} K^{-1}	λ_z Mean ± S.D., W m^{-1} K^{-1}	λ_{II}/λ_z Range	λ_{II}/λ_z Mean ± S.D.	Number of Samples
Variscan granite	3.3–3.8	3.5 ± 0.2						1.0	6
Metadiabase		3.1							1
Orthogneiss	2.4–3.4	2.8 ± 0.4	3.5–3.7	3.6 ± 0.1	2.1–3.2	2.6 ± 0.6	1.2–1.7	1.5 ± 0.2	4
Paragneiss	2.3–3.5	2.9 ± 0.4	3.5–4.5	4.0 ± 0.4	1.9–2.8	2.5 ± 0.3	1.2–2.0	1.6 ± 0.2	13
Mica schist	2.0–3.6	2.9 ± 0.7	2.6–3.8	3.2 ± 0.6	1.8–2.9	2.6 ± 0.5	1.3–1.4	1.3 ± 0.1	4
Phyllite	2.7–4.1	3.2 ± 0.7	3.3–4.7	3.9 ± 0.4	1.7–4.1	2.9 ± 0.7	1.1–1.9	1.5 ± 0.3	12
Slate	2.9–3.7	2.9 ± 0.5	3.4–3.9	3.7 ± 0.2	2.2–3.7	2.9 ± 0.8	1.1–1.7	1.3 ± 0.3	6
Pelite	2.7–3.3	2.9 ± 0.2						1.0	6

[a]Variables λ_e, effective thermal conductivity parallel to core axis; λ_{II}, parallel to foliation; λ_z, perpendicular to foliation; S.D., 1 σ standard deviation.

employed, which is based on a simulation of the temperature buildup at the bottom of the well during shut-in time. Originally, the model was derived by *Bullard* [1947] and later modified by *Lachenbruch and Brewer* [1959]. The temperature disturbance caused by the circulating mud is modeled as a line heat sink in a homogeneous borehole medium.

Generally, Bullard's equation is simplified to

$$T = T(t_s) + Q'/4k \ln [t_s/(t_s + t_c)],$$

where T is the formation equilibrium temperature, $T(t_s)$ is the bottom hole temperature (BHT) measured at shut-in time t_s, t_c is the circulation time, Q' is a modified line source strength, and k is the system (borehole mud and formation) thermal conductivity. The Horner method then is based on plotting a multiple set of single temperatures from the bottom part of the well versus $\ln [t_s/(t_s + t_c)]$, as it is usual practice in determining the pressure buildup in a well [see *Horner*, 1951; *Dowdle and Cobb*, 1975]. The term $Q'/4k$ is the slope of the Horner line, and the intercept of the line at $\ln [t_s/(t_s + t_c)] = 0$ indicates the equilibrium temperature at infinite shut-in time. In this approach the bottom hole temperature is considered equal to the circulating mud temperature and thus treated as a constant. The simplification of Bullard's equation requires that longer shut-in times be used in larger diameter wells. *Funnell et al.* [1996] show the effect of increasing bottom hole diameter on the minimum shut-in time that is necessary for linear extrapolation within a few degrees of true equilibrium temperature. The wells in this study are relatively slim with diameters ranging from 76 to 113 mm (Table 1) compared to the larger borehole diameters used, for example, in hydrocarbon exploration.

In Figure A4 repeated temperature logs are shown together with the equilibrium bottom hole temperature calculated using the Horner method. The shut-in times recorded range between 4 and 240 hours. Time of mud circulation at the well bottom is 6 hours on average. In all three situations it was observed that the temperature disturbance and the adjustment surprisingly were rather small, consequently resulting in small Horner slopes. The temperature difference at the well bottom between the first log and the Horner-corrected value is of the order of 1.0°C (Pob 2, Kt 8) and 2.7°C in the deeper Kt 34 borehole. The difference in absolute temperature of 1.0–2.7°C amounts to an average gradient difference for the logs of the order of 1.0–2.4°C km^{-1}. However, the temperature adjustment in these wells is inconsistent with their shut-in times. Only the 750-m-deep Pob 2 logs showed the expected relaxation trend of increasing temperature near total depth and decreasing temperature in the shallow part of the borehole.

Because of the sparse correction data set it is not possible to specify correction factors for all Erzgebirge logs. However, with regard to the total depth of the boreholes, which mostly is <1000 m, it is assumed that the borehole thermal conditions have almost attained equilibrium after shut-in times of between 6 and 10 days (144 and 240 hours). In comparison, the temperature relaxation toward rock equilibrium temperature observed in a somewhat deeper (1600 m) borehole in the northeast German sedimentary basin has shown that after a shut-in time of 500 hours, about 65% of total adjustment of the average temperature gradient was accomplished [*Förster*, 1997]. This amounts to a 6°C km^{-1} correction of the average gradient. The total average gradient correction required to adjust for total thermal equilibrium in the borehole is of the order of 10°C km^{-1}. Similar observations of a slower temperature adjustment after a period of fast wall rock temperature relaxation were discussed by *Sass et al.* [1992]. Considering all the facts, for the Erzgebirge an empirical gradient correction of 3°C km^{-1} was applied to logs from boreholes deeper than 500 m and shut-in times <200 hours (Table A1). This amount of correction is considered as a minimum value, but is consistent with the observations from the composite plots of temperature logs measured at different shut-in times in the different subareas studied here.

Appendix B: Thermal Conductivity Measurements

Effective thermal conductivity (Table A1) parallel to the core axis was estimated with the (1) divided-bar apparatus (error of measurement 5%) on sample disks of 30 mm diameter and 2 mm height, and the (2) optical-scanning method on half core of at least 5 cm length, both for laboratory conditions of ~20°C. With the latter method, distribution of thermal conductivity and diffusivity, coefficient of thermal heterogeneity, and main components of the conductivity tensor were determined for each sample. Error of measurement is <5% for thermal conductivities in the range of 0.2–50 W m^{-1} K^{-1} [*Popov and Pevzner*, 1994].

To correct the thermal conductivity values measured on dry air samples for water saturation, effective porosity was estimated on gneiss, phyllite, and slate samples using the Archimedian method of mass determination. Effective porosity ranged between 0.3 and 1.8%. No relation between the value

Table A2. Summary of Geothermal Data for the Erzgebirge[a]

Well Designation	Depth Interval, m	Γ_m, °C km^{-1}	T_0, °C	ST, hours	Γ_c, °C km^{-1}	λ_e, W m^{-1} K^{-1}	Major Rock Type	q_s, mW m^{-2}
Sbr 2	100–350	31.1 ± 2.7	7.7	48	···			
Sbr 4	200–400	26.8 ± 1.9	9.0	12	29.8 ± 1.9			
Sbr 5	100–450	25.7 ± 3.0	7.6	18	28.7 ± 3.0			
Sbr 6	100–500	21.4 ± 2.8	8.4	72	24.4 ± 2.8			
Sbr 7	100–550	28.7 ± 4.1	9.0	1248	···	2.9	slate (sub. metadiabase)	83.2
Sbr 8	100–400	30.6 ± 3.1	6.6	12	···			
Sbr 9	100–850	26.6 ± 6.1	9.8	164	29.6 ± 6.1			
Sbr 10	150–650	30.0 ± 4.8	8.0	48	33.0 ± 4.8			
Sbr 16	200–900	26.6 ± 5.8	8.5	30	29.6 ± 5.8			
Böu 5	100–186	27.2 ± 0.7	7.4	12	···			
Böu 9	150–350	30.2 ± 2.1	8.2	12	···	(2.9)	slate (sub. metadiabase)	87.6
Böu 16	100–715	28.0 ± 5.0	8.6	12	31.0 ± 5.0			
Böu 37	340–493	34.2 ± 1.5	6.8	12	···			
Kt 3	100–494	34.8 ± 4.0	7.7	216	···			
Kt 8	100–550	27.1 ± 3.9	6.7	42	30.1 ± 3.9			
Kt 18	400–550	24.8 ± 2.8	5.1	62	27.8 ± 2.8			
Kt 34	100–900	28.9 ± 7.1	5.1	42	31.9 ± 7.1	3.1	mica schist/phyllite	98.9
Tah 4	100–1200	23.9 ± 5.5	6.0	7	26.9 ± 5.5		greisen/granite	
	100–1000	23.0 ± 5.6			26.0 ± 5.6		greisen	
	1000–1200	28.0 ± 2.0			31.0 ± 2.0	3.6	granite	111.6
Tah 13	100–850	23.6 ± 7.5	6.2	192	26.6 ± 7.5		greisen/granite	
	100–250	25.6 ± 1.4			28.6 ± 1.4	(3.6)	granite	103.0
	250–850	23.9 ± 4.5			26.9 ± 4.5		greisen	
Zwö 1	100–700	19.2 ± 3.6	7.7	72	22.3 ± 4.5	3.2	phyllite (sub. pelite, mica schist)	71.4
Hrm 1E	280–350	21.7 ± 0.5	8.2	?	···	3.2	phyllite/mica schist (metadiabase)	69.4
Pob 1	150–450	30.1 ± 3.0	6.4	287	···	(3.0)	paragneiss/orthogneiss	90.3
	500–650	24.2 ± 1.4				(3.6)	granite	87.0
Pob 2	100–450	30.8 ± 3.5	7.3	240	···	(3.0)	orthogneiss (sub. paragneiss)	92.4
	500–750	27.4 ± 2.3				3.6	granite	98.6
Szu 1	100–600	28.9 ± 4.2	2.3	231	···	(3.0)	paragneiss/orthogneiss	86.7
	650–850	24.6 ± 2.1				(3.6)	granite	88.6
Rieg 1	100–329	23.5 ± 1.6	9.4	216	···	(3.0)	paragneiss/orthogneiss/mica schist	70.5
Grsm 1	100–286	19.1 ± 1.0	9.1	312	···	3.2	paragneiss/mica schist	61.1
Rsb 1	100–433	18.3 ± 1.8	12.6	216	21.3 ± 1.8	(3.0)	paragneiss/orthogneiss	63.9
Oba 1	120–300	23.3 ± 1.1	9.0	144	···	(3.2)	paragneiss (sub. rhyolite)	74.6

[a]Γ_m is least squares gradient over measured interval with 1σ standard deviation; Γ_c is that gradient corrected for thermal equilibrium; λ_e, effective thermal conductivity measured and corrected for water saturation, effective thermal conductivity extrapolated from nearby boreholes is given in parentheses; ST, shut-in time; q_s, surface heat flow; T_0, ambient surface temperature; sub., subordinate.

and individual rock type was observed. As a rule of thumb, an effective porosity of 1% was assumed to be a typical value for all rock types. The water-saturated thermal conductivity (λ_{wsat}) then was calculated by combining the geometric mean mixing equations for air-saturated and water-saturated thermal conductivity values as

$$\lambda_{wsat} = \lambda_{asat} x \lambda_w^{\Phi} / \lambda_a^{\Phi},$$

where λ_{asat} is the thermal conductivity of air-saturated rock, λ_w and λ_a are the thermal conductivity of water and air, respectively, and Φ is the porosity. Assuming 1% porosity as a typical effective porosity value, the ratio of the thermal conductivity of water- and air-saturated rock ($\lambda_{wsat}^{\Phi}/\lambda_{asat}^{\Phi}$) yields 1.03. This value is in the range of values known from empirical observations in sedimentary rocks [*Somerton*, 1958] but is slightly less then a ratio observed by *Woodside and Messmer* [1961] [see *Schön*, 1996]. A higher ratio of 1.2 as reported by *Reibelt* [1991] [see *Clauser and Huenges*, 1995] from a granite sample was not considered pertinent in this situation.

Appendix C: Analysis of Heat-Producing Elements

A variety of high-precision analytical techniques were used to obtain whole rock geochemical data on homogenized rock powders. Potassium was determined conventionally by wavelength dispersion X-ray fluorescence spectrometry using fused lithium tetraborate discs. In magmatic rocks, Th and U were analyzed by inductively coupled plasma mass spectrometry (ICP-MS; Perkin-Elmer/Sciex Elan Model 500) according to the method and with the precision and accuracy outlined by *Dulski* [1994]. Th and U in metamorphic rocks also were measured by ICP-MS (Fisons/VG Plasma Quad PQ 2+) as described by *Govindaraju et al.* [1994]. The analytical precision for both ICP-MS methods generally is better than 5%.

For rocks from the heat flow borehole sites, supplementary K, Th, and U measurements were performed by gamma ray spectrometry [*Huenges et al.*, 1989] using crushed rock samples of 400 g weight. The analytical uncertainty determined by comparison with rock reference material and internal laboratory standards is about twice as high as for the wet chemical analytical methods.

Appendix D: Heat Flow Determination

Table A2 provides the sites where surface heat flow (q_s) was determined. The listed q_s values were determined within some depth interval from the product of the temperature gradient (dT/dz), calculated from a least squares fit to the temperature-depth data, and the mean thermal conductivity for the

same interval (see *Blackwell and Spafford* [1987] for details). Care was taken to separate large intervals of isotropic rocks (the granite intervals) from those intervals of rocks with a strong anisotropy of thermal conductivity (the metamorphic rocks) and to check whether changes in temperature gradient are linked with the transition of rock type.

D1. Schönbrunn/Bösenbrunn (Sbr, Böu)

The boreholes are located atop a granite massif and bottom in low-grade slate with subordinate metadiabase. Temperatures measured at the Schönbrunn site yield average gradients between 24.4 and 33.0°C km^{-1}. Variable degrees of relaxation of the temperature conditions after drilling may account for some of the variability of temperature gradients. Some portion of the gradient differences also may be attributed to anisotropy of thermal conductivity in the metamorphic rocks. Temperatures obtained in well Sbr 7, at a sufficiently long shut-in time, yield an average gradient of 28.7 ± 4.1°C km^{-1}. Gradients at the Bösenbrunn site range from 27.2 to 34.2°C km^{-1}. Here the shallower Böu 9 borehole is preferred to the deeper Böu 16 for heat flow calculations, given the short shut-in time of 12 hours for the latter. Heat flow thus determined is 83 mW m^{-2} at the Sbr site and 88 mW m^{-2} at the Böu site, respectively.

D2. Klingenthal (Kt)

Temperature-depth profiles Kt 8, Kt 34, and Kt 18 (for depths below the zones of local fluid flow disturbance) were selected for thermal gradient calculations. All boreholes encountered mica schist/phyllite in the immediate vicinity to the Eibenstock granite pluton. Temperature gradients range between 27.8 and 34.8°C km^{-1}, with the variation probably caused by locally different composition of phyllites or inclination of foliation. A temperature gradient of 31.9 ± 7.1°C km^{-1} from the deepest borehole (Kt 34), where thermal conductivity was measured on rock samples from the borehole, was used to calculate heat flow and yielded 99 mW m^{-2}, the highest determined in metamorphic rocks.

D3. Tannenbergsthal (Tah)

Two boreholes penetrate the Gottesberg microgranite-rhyolite sequence, which is metasomatically altered and mineralized, and is intruded into the Eibenstock granite pluton. In both wells, heat flow was determined in the granite intervals. Corrected temperature gradients for non-greisenized and non-mineralized granite intervals are 31.0 ± 2.0 and 28.6 ± 1.4°C km^{-1}, respectively; yielding heat flow of 112 and 103 mW m^{-2}.

D4. Zwönitz/Hormersdorf (Zwö, Hrm)

The two wells are located in the marginal phyllite unit of the Erzgebirge. The average temperature gradient for the Zwö site is 22.3°C km^{-1}; the corrected gradient is similar to the gradient obtained in phyllite and mica schist in the shallower Hrm 1E well (21.7 ± 0.5°C km^{-1}). The shut-in time for this borehole is unknown; however, the intercept of the temperature profile at T_0 = 8.2°C indicates that the log was measured under quasi-steady state conditions. Heat flow values in the two wells are similar and of the order of ~70 mW m^{-2}.

D5. Satzung/Pobershau (Szu, Pob)

The wells were drilled into granites of type 3, which are overlain by paragneisses and orthogneisses. The average temperature gradients of 28.2 ± 5.7, 26.6 ± 4.2, and 27.7 ± 6.4°C km^{-1} measured in the three boreholes are similar and point to quasi-steady state conditions. Although gradients in both the metamorphic and magmatic rocks were determined, q_s values for the granite intervals are preferred because a representative thermal conductivity in these isotropic rocks can be easily determined. The heat flow ranges from 87 to 99 mW m^{-2}.

D6. Riechberg/Großschirma/Reinsberg/Obergruna (Rieg, Grsm, Rsb, Oba)

All boreholes are in the gneiss unit, with the Oba well being close to the Niederbobritzsch low-F biotite granite suite. Gradients of 23.5 ± 1.6°C km^{-1} (Rieg 1), 19.1 ± 1.0°C km^{-1} (Grsm 1), 21.3 ± 1.8°C km^{-1} (Rsb 1), and 23.3 ± 1.1°C km^{-1} (Oba 1) were determined. Heat flow calculation yields a range between 61 and 75 mW m^{-2}. The relatively great variability in q_s compared to that in the gradients again attests to difficulties in assigning effective thermal conductivities to anisotropic rocks in a structurally complicated metamorphic environment such as the Erzgebirge.

Acknowledgments. The collection of geophysical data was supported by the Geological Survey of Saxony (Sächsisches Landesamt für Umwelt und Geologie Freiberg) and the German logging company BLM GmbH Gommern. Thermal conductivity measurements were made or supervised by Y. Popov (Moscow, Russia) and C. Grissemann (Hannover). Gamma ray spectrometric determinations of U, Th, and K were performed by A. Ullner (Potsdam). D. Stromeyer (Potsdam) is thanked for his help in running the 2-D thermal models. B. Mingram (Potsdam) has provided a great number of unpublished U, Th, and K_2O analyses for metamorphic rocks from the Erzgebirge. Interpretation and modification of the gravity model benefitted from discussion with S. Choi (Berlin). Constructive reviews by R. L. Rudnick (Cambridge, Massachusetts), J. H. Sass (Flagstaff, Arizona), J. C. Mareschal (Montreal, Canada), and an anonymous referee as well as thoughtful comments by L. Rybach (Zurich, Switzerland) helped to improve the paper. D. D. Blackwell (Dallas, Texas) and E. Huenges (Potsdam) are thanked for reading a preliminary draft of the manuscript.

References

Arshavsakaya, N. I., N. E. Galdin, E. W. Karus, O. L. Kuznetsov, E. A. Lubimova, S. Y. Milanovski, V. D. Nartikoev, S. A. Semaskko, and E. V. Smirnova, Geothermic investigations, in *The Superdeep Well of the Kola Peninsula*, edited by Y. A. Kozlovsky, pp. 387–393, Springer-Verlag, New York, 1987.

Barsukov, V. L., N. T. Sokolova, and O. M. Ivanitskii, Distribution of U, Th, and K in granites of the Aue and Eibenstock massifs, Erzgebirge, Germany, *Geochem. Int.*, *34*, 1041–1056, 1996.

Barth, M. G., W. F. McDonough, and R. L. Rudnick, Tracking the budget of Nb and Ta in the continental crust, *Chem. Geol.*, *165*, 197–213, 2000.

Basham, I. R., T. K. Ball, B. Beddoe-Stephens, and U. M. Michie, Uranium-bearing accessory minerals and granite fertility, II, Studies on granites from the British Isles, in *Compte Rendu: Methodes de Prospection de l'Uranium; Symposium sur les Methodes de Prospection de l'Uranium—Examen du Programme AEN-AIEA de R & D*, pp. 398–413, Org. for Econ. Coop. and Dev., Paris, 1982.

Bayer, U., B. Lünenschloß, J. Springer, and C. von Winterfeld, Thermal modeling at an ancient orogenetic front with special regard to the uncertainty of heat-flow predictions, in *Geologic Modeling and Mapping*, edited by A. Förster and D. F. Merriam, pp. 79–93, Plenum, New York, 1996.

Bea, F., and P. Montero, Behavior of accessory phases and redistribution of Zr, REE, Y, Th, and U during metamorphism and partial melting of metapelites in the lower crust: An example from the Kinzigite Formation of Ivrea-Verbano, NW Italy, *Geochim. Cosmochim. Acta*, *63*, 1133–1153, 1999.

Behr, H.-J., H.-J. Dürbaum, P. Bankwitz, and DEKORP Research Group (B), Crustal structure of the Saxothuringian zone: Results of the deep seismic profile MVE-90 (east), *Z. Geol. Wiss.*, *22*, 647–769, 1994.

Bingen, B., D. Demaiffe, and J. Hertogen, Redistribution of rare earth

elements, thorium and uranium over accessory minerals in the course of amphibolite to granulite facies metamorphism: The role of apatite and monazite in orthogneisses from southwestern Norway, *Geochim. Cosmochim. Acta*, *60*, 1341–1354, 1996.

Birch, F., R. F. Roy, and E. R. Decker, Heat flow and thermal history in New York and New England, in *Studies of Appalachian Geology: Northern and Maritime*, edited by E. Zen et al., pp. 437–451, John Wiley, New York, 1968.

Blackwell, D. D., Regional implications of heat flow of the Snake River Plain, northwestern United States, *Tectonophysics*, *164*, 323–343, 1989.

Blackwell, D. D., and R. E. Spafford, Experimental methods in continental heat-flow, in *Geophysics, Methods Exp. Phys.*, vol. 24, Part B, edited by C. G. Sammis and T. L. Henyey, pp. 189–226, Academic, San Diego, Calif., 1987.

Broska, I., and P. Siman, The breakdown of monazite in West-Carpathian Veporic orthogneisses and Tatric granites, *Geol. Carpathica*, *49*, 161–167, 1998.

Broska, I., I. Petrík, and C. T. Williams, Coexisting monazite and allanite in peraluminous granitoids of the Tribeč Mountains, western Carpathians, *Am. Mineral.*, *85*, 22–32, 2000.

Brott, C. A., D. D. Blackwell, and J. P. Ziagos, Thermal and tectonic implications of heat flow in the Eastern Snake River Plain, Idaho, *J. Geophys. Res.*, *86*, 11,709–11,734, 1981.

Bullard, E. C., The time necessary for a borehole to attain temperature equilibrium, *Mon. Not. R. Astron. Soc., Geophys. Suppl.*, *5*, 127–130, 1947.

Čermák, V., Combined heat-flow–heat-generation measurement in the Bohemian Massif, *Geothermics*, *4*, 19–26, 1975a.

Čermák, V., Temperature-depth profiles in Czechoslovakia and some adjacent areas derived from heat flow measurements, deep seismic sounding and other geophysical data, *Tectonophysics*, *26*, 103–119, 1975b.

Čermák, V., Heat flow investigations in Czechoslovakia, in *Geophysical Syntheses in Czechoslovakia*, edited by A. Zátopek, pp. 427–439, Vedá, Bratislava, Slovakia, 1981.

Čermák, V., Crustal heat production and mantle heat flow in central and eastern Europe, *Tectonophysics*, *159*, 195–215, 1989.

Čermák, V., Lithospheric thermal regimes in Europe, *Phys. Earth Planet. Inter.*, *79*, 179–193, 1993.

Čermák, V., and L. Rybach, Vertical distribution of heat production in the continental crust, *Tectonophysics*, *159*, 217–230, 1989.

Chappell, B. W., Aluminum saturation in I- and S-type granites and the characterization of fractionated haplogranites, *Lithos*, *46*, 535–551, 1999.

Choi, S., Horizontale und vertikale Dichtezonierung in den Varisziden am Beispiel des Erzgebirges, dissertation, Freie Univ., Berlin, 2000.

Choi, S., H.-J. Götze, and O. Krentz, Gravity stripping of Paleozoic crustal domains—An example from the Erzgebirge, *Terra Nostra*, *2*, 38–42, 1998.

Clauser, C., and E. Huenges, Thermal conductivity of rocks and minerals, in *Rock Physics and Phase Relations: A Handbook of Physical Constants*, *AGU Ref. Shelf*, vol. 3, edited by T. J. Ahrens, pp. 105–126, AGU, Washington, D. C., 1995.

Clauser, C., P. Giese, E. Huenges, T. Kohl, H. Lehmann, L. Rybach, J. Safanda, H. Wilhelm, K. Windlow, and G. Zoth, The thermal regime of the crystalline continental crust: implications from the KTB, *J. Geophys. Res.*, *102*, 18,417–18,441, 1997.

Condie, K. C., Chemical composition and evolution of the upper continental crust: contrasting results from surface samples and shales, *Chem. Geol.*, *104*, 1–37, 1993.

Diener, I., et al., *Geothermie-Atlas der DDR*, 11 pp., 27 maps, Zentr. Geol. Inst., Berlin, 1984.

Dowdle, W. L., and W. M. Cobb, Static formation temperature from well logs, an empirical method, *J. Pet. Technol.*, *27*, 1326–1330, 1975.

Dubessy, J., C. Ramboz, C. Nguyen-Trung, M. Cathelineau, B. Charoy, M. Cuney, J. Leroy, B. Poty, and A. Weisbrod, Physical and chemical controls (f_{O_2}, T, pH) of the opposite behaviour of U and Sn-W as examplified by hydrothermal deposits in France and Great Britain, and solubility data, *Bull. Mineral.*, *110*, 261–281, 1987.

Dulski, P., Interferences of oxide, hydroxide, and chloride analyte species in the determination of rare earth elements in geological samples by inductively coupled plasma-mass spectrometry, *Fresenius J. Anal. Chem.*, *350*, 194–203, 1994.

Dunai, T. J., and H. Baur, Helium, neon, and argon systematics of the European subcontinental mantle: Implications for its geochemical evolution, *Geochim. Cosmochim. Acta*, *59*, 2767–2783, 1995.

Eby, G. N., The A-type granitoids: A review of their occurrence and chemical characteristics and speculations on their petrogenesis, *Lithos*, *26*, 115–134, 1990.

England, P. C., E. R. Oxburgh, and S. W. Richardson, Heat refraction in and around granite plutons in north-east England, *Geophys. J. R. Astron. Soc.*, *62*, 439–455, 1980.

Finger, F., I. Broska, M. Roberts, and A. Schermaier, Replacement of primary monazite by apatite-allanite-epidote coronas in an amphibolite facies granite gneiss from the eastern Alps, *Am. Mineral.*, *83*, 248–258, 1998.

Förster, A., Bewertung der geothermischen Bedingungen im Ostteil des Norddeutschen Beckens, in *Geothermie Report 97-1: Geowissenschaftliche Bewertungsgrundlagen zur Nutzung hydrogeothermaler Ressourcen in Norddeutschland*, edited by P. Hoth et al., pp. 20–41, *Sci. Tech. Rep. STR97/15*, GeoForschungsZentrum Potsdam, Potsdam, Germany, 1997.

Förster, H.-J., Die variszischen Granite des Erzgebirges und ihre akzessorischen Minerale, Habilitation thesis, Tech. Univ. Bergakad., Freiberg, Germany, 1998.

Förster, H.-J., The chemical composition of uraninite in Variscan granites of the Erzgebirge, Germany, *Mineral. Mag.*, *63*, 239–252, 1999.

Förster, H.-J., Cerite-(Ce) and thorian synchysite-(Ce) from the Niederbobritzsch granite (Erzgebirge, Germany): Implications for the differential mobility of the LREE and Th during alteration, *Can. Mineral.*, *38*, 67–79, 2000.

Förster, H.-J., and G. Tischendorf, Reconstruction of the volatile characteristics of granitoidic magmas and hydrothermal solutions on the basis of dark micas: The Hercynian postkinematic granites and associated high-temperature mineralizations of the Erzgebirge (G.D.R.): Calculation procedure and results, *Chem. Erde*, *49*, 7–20, 1989.

Förster, H.-J., G. Tischendorf, R. Seltmann, and B. Gottesmann, Die variszischen Granite des Erzgebirges: Neue Aspekte aus stofflicher Sicht, *Z. Geol. Wiss.*, *26*, 31–60, 1998.

Förster, H.-J., G. Tischendorf, R. B. Trumbull, and B. Gottesmann, Late-collisional granites in the Variscan Erzgebirge, *J. Petrol.*, *40*, 1613–1645, 1999.

Fricke, S., and P. Schlosser, Probleme der Ermittlung von Gesteinstemperaturen durch Bohrlochmessungen in übertiefen Bohrlöchern der DDR, *Z. Angew. Geol.*, *26*, 619–623, 1980.

Frost, C. D., B. R. Frost, K. R. Chamberlain, and B. R. Edwards, Petrogenesis of the 1.43 Ga Sherman batholith, SE Wyoming, USA: A reduced, rapakivi-type anorogenic granite, *J. Petrol.*, *40*, 1771–1802, 1999.

Frottier, L. G., J.-C. Mareschal, C. Jaupart, C. Gariépy, R. Lapointe, and G. Bienfait, Heat flow variations in the Grenville Province, Canada, *Earth Planet. Sci. Lett.*, *136*, 447–460, 1995.

Funnell, R. H., R. G. Allis, D. S. Chapman, and P. A. Armstrong, Thermal regime of the Taranaki basin, New Zealand, *J. Geophys. Res.*, *101*, 25,197–25,215, 1996.

Furlong, K. P., and D. S. Chapman, Crustal heterogeneities and the thermal structure of the continental crust, *Geophys. Res. Lett.*, *14*, 314–317, 1987.

Gottesmann, B., R. Seltmann, and H.-J. Förster, Felsic subvolcanic intrusions within the Eibenstock granite pluton (Saxony, Germany): The Gottesberg volcano-plutonic system, *Terra Nostra*, *7*, 49–53, 1995.

Govindaraju, K., P. J. Potts, P. C. Webb, and J. S. Watson, Report on Whin Sill dolerite WS-E from England and Pitscurrie microgabbro from Scotland, *Geostand. Newsl.*, *18*, 211–300, 1994.

Hansen, E. C., R. C. Newton, A. S. Janardhar, and S. Lindenberg, Differentiation of Late Archean crust in the eastern Dharwar Craton, Krishnagiri-Salem area, south India, *J. Geol.*, *103*, 629–651, 1995.

Horner, D. R., Pressure build-up in wells, in *Proceedings of the Third World Petroleum Congress, The Hague, sect. II*, pp. 503–521, E. J. Brill, Cologne, Germany, 1951.

Huenges, E., C. Bücker, K. E. Wolter, J. Wienand, A. Rauen, and E. Lippmann, Deep drilling KTB Oberpfalz VB results of the geoscientific proceedings in the KTB-laboratory; depth interval: 1709 to 2500 m, *KTB Rep. 89-2*, pp. D1–D83, Niedersächsisches Landesamt für Bodenforsch., Hannover, Germany, 1989.

Hurtig, E., and C. Oelsner, The heat flow field on the territory of the

German Democratic Republic, in *Terrestrial Heat Flow in Europe*, edited by V. Čermak and L. Rybach, pp. 186–190, Springer-Verlag, New York, 1979.

Hurtig, E., and W. Rockel, Federal Republic of Germany, eastern states, in *Geothermal Atlas of Europe*, edited by E. Hurtig et al., pp. 38–40, Hermann Haak, Gotha, Germany, 1992.

Irber, W., The lanthanide tetrad effect and its correlation with K/Rb, Eu/Eu*, Sr/Eu, Y/Ho, and Zr/Hf of evolving peraluminous granite suites, *Geochim. Cosmochim. Acta*, *63*, 489–508, 1999.

Jaupart, C., Horizontal heat transfer due to radioactivity contrasts: Causes and consequences of the linear heat flow relation, *Geophys. J. R. Astron. Soc.*, *75*, 411–435, 1983.

Jaupart, C., and J. C. Mareschal, The thermal structure and thickness of continental roots, *Lithos*, *48*, 93–114, 1999.

Jolivet, J., G. Bienfait, J. L. Vigneresse, and M. Cuney, Heat flow and heat production in Brittany (western France), *Tectonophysics*, *159*, 61–72, 1989.

Kontak, D. J., The East Kemptville topaz-muscovite leucogranite, Nova Scotia, I, Geological setting and whole-rock geochemistry, *Can. Mineral.*, *28*, 787–825, 1990.

Kopf, M., Dichtewerte von Gesteinen des Erzgebirges und der angrenzenden Gebiete, *Z. Angew. Geol.*, *6*, 301–302, 1961.

Kröner, A., and A. P. Willner, Time of formation and peak of Variscan HP-HT metamorphism of quartz-feldspar rocks in the central Erzgebirge, Saxony, Germany, *Contrib. Mineral. Petrol.*, *132*, 1–20, 1998.

Kukkonen, I. T., Thermal aspects of groundwater circulation in bedrock and its effect on crustal geothermal modelling in Finland, the central Fennoscandian Shield, *Tectonophysics*, *244*, 119–136, 1995.

Kukkonen, I. T., and J. Šafanda, Paleoclimate and structure: The most important factors controlling subsurface temperatures in crystalline rocks. A case history from Outokumpu, eastern Finland, *Geophys. J. Int.*, *126*, 101–112, 1996.

Kuschka, E., and W. Hahn, *Flußspatlagerstätten des Südwestvogtlandes: Schönbrunn, Bösenbrunn, Wiedersberg, Bergbaumonogr. Bergbau in Sachsen*, vol. 2, 283 pp., Landesamt für Umwelt und Geol., Oberbergamt des Freistaates Sachsen, Freiberg, Germany, 1996.

Lachenbruch, A. H., Preliminary geothermal model of the Sierra Nevada, *J. Geophys. Res.*, *73*, 6977–6989, 1968.

Lachenbruch, A. H., Crustal temperature and heat production: Implications of the linear heat flow relation, *J. Geophys. Res.*, *75*, 3291–3300, 1970.

Lachenbruch, A. H., and M. C. Brewer, Dissipation of the temperature effect of drilling a well in arctic Alaska, *U.S. Geol. Surv. Bull.*, *1083C*, 73–109, 1959.

Lachenbruch, A. H., and J. H. Sass, Heat flow in the United States and the thermal regime of the crust, in: *The Earth's Crust*, *Geophys. Monogr. Ser.*, vol. 20, edited by J. H. Heacock, pp. 626–675, AGU, Washington, D. C., 1977.

Lee, M. K., J. Wheildon, P. C. Webb, G. C. Brown, I. F. Smith, G. King, A. Thomas-Betts, K. E. Rollin, and C. N. Crook, Hot dry rock prospects in Caledonian granites: Evaluation of results from BGS-IC-OU research programme (1981–1984), 83 pp., Brit. Geol. Surv., Keyworth, England, 1984.

Lee, M. K., G. C. Brown, P. C. Webb, J. Wheildon, and K. E. Rollin, Heat flow, heat production and thermo-tectonic setting in mainland UK, *J. Geol. Soc. London*, *144*, 35–42, 1987.

Mareschal, J. C., C. Jaupert, L. Z. Cheng, F. Rolandone, C. Gariépy, G. Bienfait, L. Guillou-Frottier, and R. Lapointe, Heat flow in the Trans-Hudson Orogen of the Canadian Shield: Implications for Proterozoic continental growth, *J. Geophys. Res.*, *104*, 29,007–29,024, 1999.

Matte, P., H. Maluski, P. Rajlich, and W. Franke, Terrane boundaries in the Bohemian Massif: Result of large-scale Variscan shearing, *Tectonophysics*, *177*, 151–170, 1990.

McDonough, W. F., Constraints on the composition of the continental lithospheric mantle, *Earth Planet. Sci. Lett.*, *101*, 1–18, 1990.

McLennan, S. M., and S. R. Taylor, Heat flow and the chemical composition of continental crust, *J. Geol.*, *104*, 369–377, 1996.

Mingram, B., Geochemische Signaturen der Metasedimente des erzgebirgischen Krustenstapels, *Sci. Tech. Rep. STR 96/04*, 104 pp., GeoForschungsZentrum Potsdam, Potsdam, Germany, 1996.

Mingram, B., The Erzgebirge, Germany, a subducted part of northern Gondwana: geochemical evidence for repetition of early Palaeozoic metasedimentary sequences in metamorphic thrust units, *Geol. Mag.*, *135*, 785–801, 1998.

Morgan, P., The thermal structure and thermal evolution of the continental lithosphere, *Phys. Chem. Earth*, *15*, 107–193, 1984.

Morgan, P., Crustal radiogenic heat production and the selective survival of ancient continental crust, *Proc. Lunar Planet. Sci. Conf. 15th*, Part 2, *J. Geophys. Res.*, *90*, suppl., C561–C570, 1985.

Morgan, P., and W. D. Gosnold, Heat flow and thermal regimes in the continental United States, *Mem. Geol. Soc. Am.*, *172*, 493–522, 1989.

Müller, A., G. Stiehl, T. Böttger, H.-K. Bothe, O. Gebhardt, M. Geisler, D. Haendel, H.-M. Nitzsche, and E. Schmädicke, Geochemical, stable isotope and petrographic investigations of granulites, pyriclasites and metagranulitic rocks of the Sächsisches Granulitgebirge, in *Contributions to the Geology of the Saxonian Granulite Massif (Sächsisches Granulitgebirge)*, edited by H. Gerstenberger, *Mitt. 133*, pp. 145–205, Zentralinst. für Isotopen- und Strahlenforsch., Leipzig, Germany, 1987.

Nyblade, A. A., and H. N. Pollack, A global analysis of heat flow from Precambrian terrains: Implications for the thermal structure of Archean and Proterozoic lithosphere, *J. Geophys. Res.*, *98*, 12,207–12,218, 1993.

Oelsner, C., Ergebnisse der Berechnung eines geothermischen Schnittes im Bereich des Erzgebirges in Abhängigkeit von Eingabedaten, *Stud. Geophys. Geod.*, *22*, 190–196, 1978.

Oelsner, C., and E. Hurtig, Zur geothermischen Situation im Erzgebirge, *Freiberg. Forschungsh. C*, *350*, 7–17, 1979.

Ostřihanský, L., The structure of the Earth's crust and the heat-flow–heat-generation relationship in the Bohemian Massif, *Tectonophysics*, *68*, 325–337, 1980.

Ostřihanský, L., The structure of the Earth's crust and the heat-flow–heat-generation relationship in the Bohemian Massif, in *Proceedings of the 1st International Conference on the Bohemian Massif*, edited by Z. Kukal, pp. 210–217, Czech Geol. Surv., Prague, 1988.

Pinet, C., C. Jaupart, J.-C. Mareschal, C. Gariepy, G. Bienfait, and R. Lapointe, Heat flow and structure of the lithosphere in the eastern Canadian Shield, *J. Geophys. Res.*, *96*, 19,941–19,963, 1991.

Poitrasson, F., S. Chenery, and D. J. Bland, Contrasted monazite hydrothermal alteration mechanisms and their geochemical implications, *Earth Planet. Sci. Lett.*, *145*, 79–96, 1996.

Pollack, H. N., S. J. Hurter, and J. R. Johnson, Heat flow from the Earth's interior; analysis of the global data set, *Rev. Geophys.*, *31*, 267–280, 1993.

Polyak, B. G., E. M. Prasolov, V. Čermák, and A. B. Verkhovskiy, Isotopic composition of noble gases in geothermal fluids of the Krušné hory Mts., Czechoslovakia, and the nature of the local geothermal anomaly, *Geochim. Cosmochim. Acta*, *49*, 695–699, 1985.

Popov, Y. A., and L. A. Pevzner, Vertical variation in heat flow density and rock thermal properties along the scientific boreholes of Russia, in *Proceedings of the VIIth International Symposium on the Observation of the Continental Crust Through Drilling*, pp. 269–272, DOSECC Inc., Santa Fe, N. M., 1994.

Popov, Y. A., D. F. C. Pribnow, J. H. Sass, C. F. Williams, and H. Burkhardt, Characterization of rock thermal conductivity by high-resolution optical scanning, *Geothermics*, *28*, 253–276, 1999.

Rao, R. U. M., G. V. Rao, and G. K. Reddy, Age dependence of continental heat flow; fantasy and fact, *Earth Planet. Sci. Lett.*, *59*, 288–302, 1982.

Reibelt, M., Study of the influence of surface structure and fluid-saturation of rocks on the determination of thermal conductivity using the half-space line source (Untersuchung des Einflusses der Oberflächenbeschaffenheit und der Fluidsättigung von Gesteinen auf die Messung der Wärmeleitfähigkeit mit einer Halbraumlinienquelle), Diploma thesis, Tech. Univ., Berlin, 1991.

Rötzler, K., R. Schumacher, W. V. Maresch, and A. P. Willner, Characterization and geodynamic implications of contrasting metamorphic evolution in juxtaposed high-pressure units of the western Erzgebirge (Saxony, Germany), *Eur. J. Mineral.*, *10*, 261–280, 1998.

Roy, R. F., D. D. Blackwell, and F. Birch, Heat generation of plutonic rocks and continental heat flow provinces, *Earth Planet. Sci. Lett.*, *5*, 1–12, 1968.

Rudnick, R. L., and D. M. Fountain, Nature and composition of the continental crust: A lower crustal perspective, *Rev. Geophys.*, *33*, 267–309, 1995.

Rudnick, R. L., W. F. McDonough, and R. J. O'Connell, Thermal structure, thickness and composition of continental lithosphere, *Chem. Geol.*, *145*, 395–411, 1998.

Rybach, L., Wärmeproduktionsbestimmungen an Gesteinen der Schweizer Alpen, *Beitr. Geol. Schweiz, Geotech. Ser.*, *51*, 43 pp., 1973.

Rybach, L., and G. Buntebarth, Heat-generating radioelements in granitic magmas, *J. Volcanol. Geotherm. Res.*, *10*, 395–404, 1981.

Sächsisches Landesamt für Umwelt und Geologie, Geologische Übersichtskarte des Freistaates Sachsen, scale 1:400000, 1 sheet, Freiberg, Germany, 1995.

Sass, J. H., A. H. Lachenbruch, T. H. Moses Jr., and P. Morgan, Heat flow from a scientific research well at Cajon Pass, California, *J. Geophys. Res.*, *97*, 5017–5030, 1992.

Schön, J. H., *Physical Properties of Rocks: Fundamentals and Principles of Petrophysics, Handb. Geophy. Explor., Sect. 1, Seismic Explor.*, vol. 18, edited by K. Helbig and S. Teitel, pp. 323–378, Pergamon, Tarrytown, N. Y., 1996.

Shaw, D. M., J. J. Cramer, M. D. Higgins, and M. G. Truscott, Composition of the Canadian Precambrian shield and the continental crust of the Earth, in *The Nature of the Lower Continental Crust*, edited by J. B. Dawson et al., *Geol. Soc. Spec. Publ.*, *24*, 257–282, 1986.

Somerton, W. H., Some thermal characteristics of rocks, *Trans. AIME*, *213*, 375–378, 1958.

Taylor, R. P., Petrological and geochemical characteristics of the Pleasant Ridge zinnwaldite-topaz granite, southern New Brunswick, and comparisons with other topaz-bearing felsic rocks, *Can. Mineral.*, *30*, 895–921, 1992.

Taylor, S. R., and S. M. McLennan, *The Continental Crust: Its Composition and Evolution*, 312 pp., Blackwell, Malden, Mass., 1985.

Tischendorf, G., and H.-J. Förster, Hercynian granite magmatism and related metallogenesis in the Erzgebirge: a status report, in *Mineral Deposits of the Erzgebirge/Krušné hory (Germany/Czech Republic)*, edited by K. von Gehlen and D. D. Klemm, pp. 5–23, Gebrüder Bornträger, Berlin, 1994.

Tischendorf, G., J. Wasternack, H. Bolduan, and E. Bein, Zur Lage der Granitoberfläche im Erzgebirge und Vogtland mit Bemerkungen über ihre Bedeutung für die Verteilung endogener Lagerstätten, *Z. Angew. Geol.*, *11*, 410–423, 1965.

Tomek, F. H., V. Dvorakva, and S. Vrana, Geological interpretation of the 9HR and 503M seismic profiles in western Bohemia, *J. Geol. Sci.*, *47*, 43–50, 1997.

Ulrych, J., and E. Pivec, Age-related contrasting alkaline volcanic series in north Bohemia, *Chem. Erde*, *57*, 311–336, 1997.

Vigneresse, J. L., Forme et volume des plutons granitiques, *Bull. Soc. Geol. Fr.*, *8*, 897–906, 1988.

Vigneresse, J. L., Thermal data and crustal structure: Role of granites and the depleted lower crust, in *Granulites and Crustal Evolution*, edited by D. Vielzeuf and P. Vidal, pp. 551–568, Kluwer Acad., Norwell, Mass., 1990.

Vigneresse, J. L., Intrusion level of granitic massifs along the Hercynian belt: Balancing the eroded crust, *Tectonophysics*, *307*, 277–295, 1999.

Vigneresse, J. L., and M. Cuney, Are granites representative of heat flow provinces?, in *Terrestrial Heat Flow and the Lithosphere Structure*, edited by V. Čermák and L. Rybach, pp. 86–110, Springer-Verlag, New York, 1991.

Vigneresse, J. L., M. Cuney, J. Jolivet, and G. Bienfait, Selective heat-producing element enrichment in a crustal segment of the mid-European Variscan chain, *Tectonophysics*, *159*, 47–60, 1989.

Vitorello, I., and H. N. Pollack, On the variation of continental heat flow with age and the thermal evolution of continents, *J. Geophys. Res.*, *85*, 983–995, 1980.

Wagner, S., Geothermische Krustenmodellierung im Südteil der DDR, *Z. Angew. Geol.*, *35*, 1–3, 1989.

Wasternack, J., S. Märtens, and B. Gottesmann, Field and petrographic study of brecciation and greisenization phenomena in the Gottesberg tin deposit (Saxony), *Z. Geol. Wiss.*, *23*, 619–642, 1995.

Webb, P. C., A. G. Tindle, S. D. Barritt, G. C. Brown, and J. F. Miller, Radiothermal granites of the United Kingdom: comparison of fractionation patterns and variation of heat production for selected granites, in *High Heat Production (HHP) Granites, Hydrothermal Circulation and Ore Genesis*, pp. 409–424, Inst. of Min. and Metall., London, 1985.

Webb, P. C., M. K. Lee, and G. C. Brown, Heat flow-heat production relationships in the UK and the vertical distribution of heat production in granite batholiths, *Geophys. Res. Lett.*, *14*, 279–282, 1987.

Weinlich, F., K. Bräuer, H. Kämpf, G. Strauch, J. Tesař, and S. M. Weise, An active subcontinental mantle volatile system in the western Eger rift, central Europe: Gas flux, isotopic (He, C, and N) and compositional fingerprints, *Geochim. Cosmochim. Acta*, *63*, 3653–3671, 1999.

Whalen, J. B., K. L. Currie, and B. W. Chappell, A-type granites: Geochemical characteristics, discrimination and petrogenesis, *Contrib. Mineral. Petrol.*, *95*, 407–419, 1987.

Willner, A. P., K. Rötzler, and W. V. Maresch, Pressure-temperature and fluid evolution of quartzo-feldspatic metamorphic rocks with a relic high-pressure, granulite facies history from the central Erzgebirge (Saxony/Germany), *J. Petrol.*, *38*, 307–336, 1997.

Woodside, W., and J. Messmer, Thermal conductivity of porous media, *J. Appl. Phys.*, *32*, 1688–1706, 1961.

Ziagos, J. P., D. D. Blackwell, and F. Mooser, Heat flow in southern Mexico and the thermal effects of subduction, *J. Geophys. Res.*, *90*, 5410–5420, 1985.

A. Förster and H.-J. Förster, GeoForschungsZentrum Potsdam, Telegraftenberg, D-14473 Potsdam, Germany. (for@gfz-potsdam.de; forhj@gfz-potsdam.de)

(Received January 25, 2000; revised June 15, 2000;
accepted July 17, 2000.)